BOLT BERANEK AND NEWMAN Inc.
CONSULTING DEVELOPMENT RESEARCH

NR-72

ACOUSTICAL AND VIBRATIONAL PERFORMANCE OF FLOATING FLOORS

Istvan L. Ver

16 October 1969

CAMBRIDGE NEW YORK CHICAGO LOS ANGELES

TIR – 72

15 October 1969

ACOUSTICAL AND VIBRATIONAL PERFORMANCE OF FLOATING FLOORS

István L. Vér

BOLT BERANEK AND NEWMAN INC.
50 Moulton Street
Cambridge, Massachusetts 02138

TABLE OF CONTENTS

LIST OF FIGURES

LIST OF SYMBOLS

A = surface area

c_0 = propagation velocity of sound in air

c_L = propagation velocity of compression waves in the solid material

d_0 = thickness of the air cushion

dB = decibel

E_a = acoustical energy in the source room

E_s = vibration energy in the slab

E = Young's modulus

F = Force

f = frequency

f_c = coincidence frequency

f_0 = resonance frequency

g = acceleration of gravity

h = slab thickness

$i = \sqrt{-1}$

k = stiffness

k_0 = stiffness of the trapped air per unit floor area

$K_{12}(\omega)$ = factor defined in Eq. 22b

ℓ = length

m = mass
m_0 = total mass of the air in the source room
m_s = total mass of the slab

n_a = acoustical modal density
n_s = structural modal density
n' = number of vibration mounts per unit slab area

p = sound pressure
p_0 = static pressure
P_r = radiating perimeter
PWL = sound power level in dB re 10^{-12} watts

$r = \frac{k}{\omega}\eta$ = real part of the mount impedance

SPL = sound pressure level in dB re 0.0002μbar

TL = sound transmission loss
TL_f = flanking sound transmission loss

v = velocity amplitude
V = volume

W_s = surface weight

x = displacement
$\ddot{x}$ = acceleration

Y = point input admittance of the slab
Y_∞ = point input admittance of an infinite slab

Z = impedance of the vibration mount

α = phase difference between the force and acceleration signal

γ = velocity transmission factor defined in Eq. 95

ΔTL = increase in TL obtained by adding the floating floor to the structural floor

η = loss factor
η_s = loss factor of the slab
η_{as} = coupling loss factor (acoustic to structure)

θ = angle of sound incidence (normal incidence = 0°)

κ = ratio of specific heats

λ = wavelength
λ_c = wavelength at coincidence frequency
λ_{ac} = acoustical wavelength

π = power

ρ_0 = mass density of air

ρ_s = surface mass density of the slab

σ_{rad} = radiation efficiency

ω = angular frequency

log( ) = refers to the ten-base logarithm of the enclosed number

Re{ } = refers to the real part of the enclosed symbol;
< > indicates spatial average of the enclosed symbol

* as superscript indicating the complex conjugate

Subscripts: 1 refers to the floating slab
2 refers to the structural slab

I. SUMMARY

The purpose of the investigations described in this report was to provide better understanding of the acoustical and vibrational performance of floating floors and to use the knowledge gained for the preparation of design charts.

The behavior of the sound and vibration transmission of floating floors in the low-frequency and high-frequency ranges were analyzed separately. In the low-frequency region, the basic resonance frequency, above which excess attenuation[a] becomes possible, was calculated. The high-frequency behavior was investigated by the statistical energy analysis method.

In order to evaluate the theoretical results, we measured the dynamic stiffness and loss factors of various commonly used resilient mounts. For all measured mounts, the dynamic stiffness was found to be frequency independent and to increase with increasing static load.

The theoretical investigation showed that the lowest possible basic resonance is given by the surface mass of the floating floor and the stiffness of the trapped air cushion. It is demonstrated that properly loaded neoprene, precompressed glass fiber, or cork mounts, being nearly as soft as the trapped air, enable one to approach this basic resonance frequency.

Well above the basic resonance frequency, the excess sound transmission loss obtained by adding the floating slab increases with a slope of 30 dB/decade.

---

[a] The excess attenuation is the increase in attenuation obtained by adding a resiliently supported slab on to the existing floor.

This large potential excess attenuation can be only partially realized because of unavoidable flanking transmission through the walls common to the source and receiving rooms. A simple engineering procedure is suggested for estimating the flanking transmission.

II. INTRODUCTION

In order to increase the sound transmission loss (TL) of a structural floor, it is customary to add a second slab supported on resilient mounts. The resilient mount can be a continuous resilient layer, such as a glass fiber blanket, cork layer, etc., or may consist of individual isolators, such as steel springs, cork, neoprene, or precompressed glass-fiber unit mounts, suitably spaced.

In the analysis of the low frequency behavior of the floating slab, we consider the surface mass of the floor, the combined stiffness of the supporting mount, and the enclosed airspace as lumped parameters. In the high frequency regime the effect of the various modes excited in the floor is analyzed by statistical methods. In both cases we calculate first the TL of the structural slab alone and then the TL of the entire floating slab system. The difference between the two TLs provides the excess transmission loss ΔTL gained by the addition of the resiliently supported second slab.

A knowledge of the basic resonance frequency and the high frequency asymptotic slope of ΔTL vs. frequency permits a simple engineering estimate of the transmission loss gain ΔTL. The detailed analysis also provides useful information about the relative importance of the design parameters.

The ΔTL calculated in this manner can be regarded as the maximum possible value that can be obtained by the addition of a floating floor. In practice flanking transmission through walls common to source and receiving room tends to reduce ΔTL and we indicate how this reduction can be estimated.

III. LOW FREQUENCY BEHAVIOR

In the design of floating floors one frequently overlooks the fact that the dynamic stiffness of the air cushion trapped between the two slabs in many cases exceeds the stiffness of the resilient mounts. Consequently, the desired low basic resonance frequencies, predicted from the surface mass of the supported slab and the stiffness of the mount alone, are not realized in many installations.

In order to illustrate this limitation, we calculate the resonance frequency that is obtained when only the air cushion provides the stiffness. This frequency is the lowest possible.

Sketch SK-1 shows a section of the floated floor system:

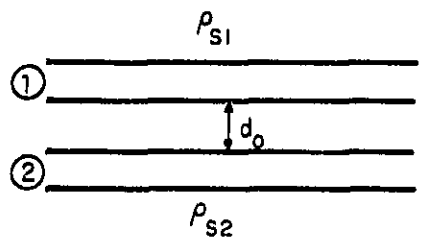

SK-1. Section of the floated floor system.

ρ_{s1} = surface mass of slab 1

ρ_{s2} = surface mass of slab 2

d_0 = thickness of air cushion

The pressure in the air cavity is given in Eq. 1:

$$p = p_0 \left(\frac{V_0}{V}\right)^{\kappa}, \qquad (1)$$

where the symbols are as follows:

p_0 = static pressure

$V_0 = d_0 A$ = static volume

A = surface area of the slab

V = instantaneous volume

κ = ratio of specific heats

(κ = 1.4 air for adiabatic compression and κ = 1 for isothermal compression.)[a]

The dynamic pressure, $p_\sim$, can be calculated by differentiating Eq. 1 with respect to V:

$$\frac{dp}{dV} = -p_0 \kappa V_0^{\kappa} V^{-(\kappa+1)} \tag{2}$$

$$p_\sim = dp = -p_0 \kappa \frac{dV}{V} . \tag{3}$$

The dynamic force F' acting on unit area of both slabs is

$$F' = p_\sim = -p_0 \kappa \frac{dV}{V} . \tag{4}$$

If the displacement amplitude causing the compression is x, then $V_0 = d_0 A$ and $dV = -xA$.

Accordingly,

$$F' = k_0 x = \frac{p_0 \kappa}{d_0} x \tag{5}$$

gives the dynamic stiffness k_0 per unit area of the air cushion:

$$k_0 = \frac{p_0 \kappa}{d_0} . \tag{6}$$

---

[a] If the entire airspace is filled with glass fiber, the compression process becomes isothermal at low frequencies (below 50 Hz), and κ=1 indicating 40% more compressibility than the adiabatic process [1].

For a completely rigid structural slab and harmonic motion of the floating slab, the external force F' must balance the inertial force of the slab and the restoring force of the compressed air cushion. The balance of forces for unit area of the slab is

$$F' = -\omega^2 \rho_{s_1} x + \frac{p_0 \kappa}{d_0} x . \qquad (7)$$

The frequency at which motion can be sustained in the absence of an outside force follows from Eq. 7 by putting F=0 and solving for ω:

$$\omega_{00} = \sqrt{\frac{p_0 \kappa}{d_0 \rho_{s_1}}} . \qquad (8)$$

For a slab of surface weight W_{s_1}, $\rho_s = W_{s_1}/g$, where g is the acceleration of gravity. The resonance frequency is then

$$f_{00} = \frac{1}{2\pi} \sqrt{\frac{p_0 \kappa g}{d_0 W_{s_1}}} . \qquad (9)$$

In deriving Eq. 9, we assumed a completely rigid *structural* slab. In practice, however, though the structural slab is usually a heavier, stiffer structure than the floating slab, it cannot be considered completely rigid. For a conservative estimate, we assume that it has a mass-like behavior. Consequently, the surface weight W_s in Eq. 9 should be replaced by $W_s = (W_{s_1} W_{s_2})/(W_{s_1} + W_{s_2})$, where W_{s_2} is the surface weight of the structural slab. This modifies the resonance frequency somewhat:

$$f_{00} = \frac{1}{2\pi}\sqrt{\frac{p_0 \kappa g}{d_0 W_s}} = \frac{1}{2\pi}\sqrt{\frac{k_0 g}{W_s}} \ . \qquad (10)$$

Using the following constants:

$$p_0 = 2.12 \times 10^3 \text{ lb/ft}^2$$

$$g = 32.2 \text{ ft/sec}^2$$

$$\kappa = 1.4 \text{ for adiabatic compression}$$

$$\kappa = 1 \text{ for isothermal compression,} \qquad (11)$$

we obtain the following formula for the lowest possible resonance frequency due to the stiffness of the enclosed air volume alone:

$$f_{00} = \frac{171}{\sqrt{d_0 W_s}} \text{ for adiabatic compression ,} \qquad (12a)$$

$$f_{00} = \frac{140}{\sqrt{d_0 W_s}} \text{ for isothermal compression .} \qquad (12b)$$

W_s is the equivalent *surface weight* in lb/ft^2 and d_0, the thickness of the airspace in inches. (Isothermal compression occurs when the airspace is filled with glass fiber, and adiabatic compression, when the airspace is free.) Equation 12a is shown in graphical form in Fig. 1. For isothermal compression, the resonance frequency read in Fig. 1 should be multiplied by 0.85.

If the floating slab is supported on resilient mounts, each having stiffness k, and the number of mounts per unit surface area is n', the resulting stiffness per unit area, k_{res}, is increased to

$$k_{res} = k_0 + n'k \ , \qquad (13)$$

and the resulting increased resonance frequency f_0 is given by

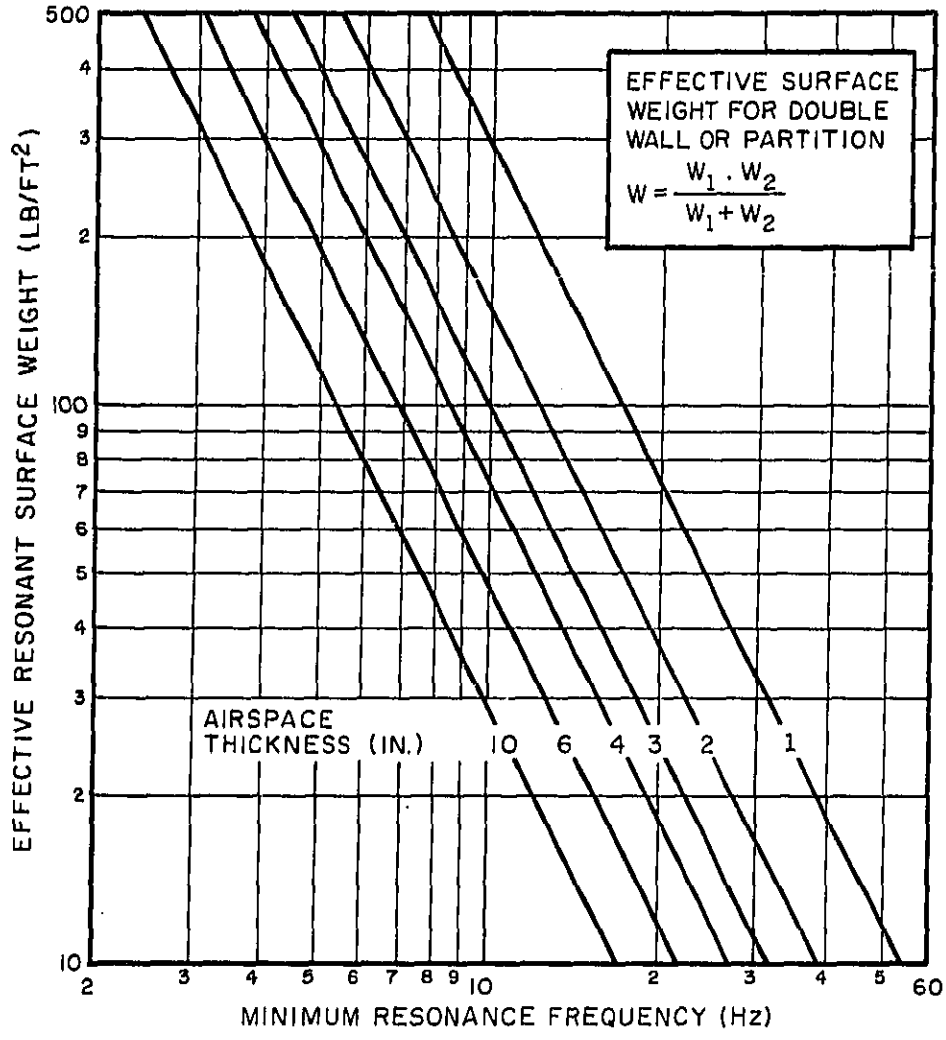

FIG. 1 MINIMUM RESONANCE FREQUENCY AS A FUNCTION OF THE EFFECTIVE SURFACE WEIGHT WITH THE THICKNESS OF THE AIRSPACE AS PARAMETER (MULTIPLY THE RESONANCE FREQUENCY BY 0.85 IF THE AIRSPACE IS FILLED WITH GLASS FIBER)

$$f_0 = \frac{1}{2\pi}\sqrt{\frac{(k_0+n'k)g}{W_s}} \qquad (14a)$$

or

$$f_0 = f_{00}\sqrt{1+\frac{n'k}{k_0}} \quad . \qquad (14b)$$

For convenience in comparing the stiffnesses, the formulas for k_0 are

$$k_0 \approx \frac{3.10^3}{d_0} \text{ for adiabatic compression} \qquad (15a)$$

and

$$k_0 \approx \frac{2.14\ 10^3}{d_0} \text{ for isothermal compression,} \qquad (15b)$$

where k_0 is the stiffness of the air cushion per sq ft of floor area in lb/in. per ft^2, and d_0 is the thickness of the airspace in inches. Equations 15a and 15b are shown in graphical form in Fig. 2.[a]

It is clear from Eq. 14b that making the resilient mounts much softer than the enclosed air ($n'k \ll k_0$) does not decrease the basic resonance frequency significantly.

As a practical example, the basic resonance frequency, f_0, for a slab of 50 lb/ft^2 equivalent surface weight and 2-in. thick airspace without glass fiber cannot be reduced below a limiting value (see Eq. 12a) of $f_{00} = 17.1$ Hz. If the stiffness of the enclosed

[a] In drawing up the right-hand scale in Fig. 2, we used the simplified relation 1m^2 = 10 ft^2, instead of the accurate 1m^2 = 10.76 ft^2.

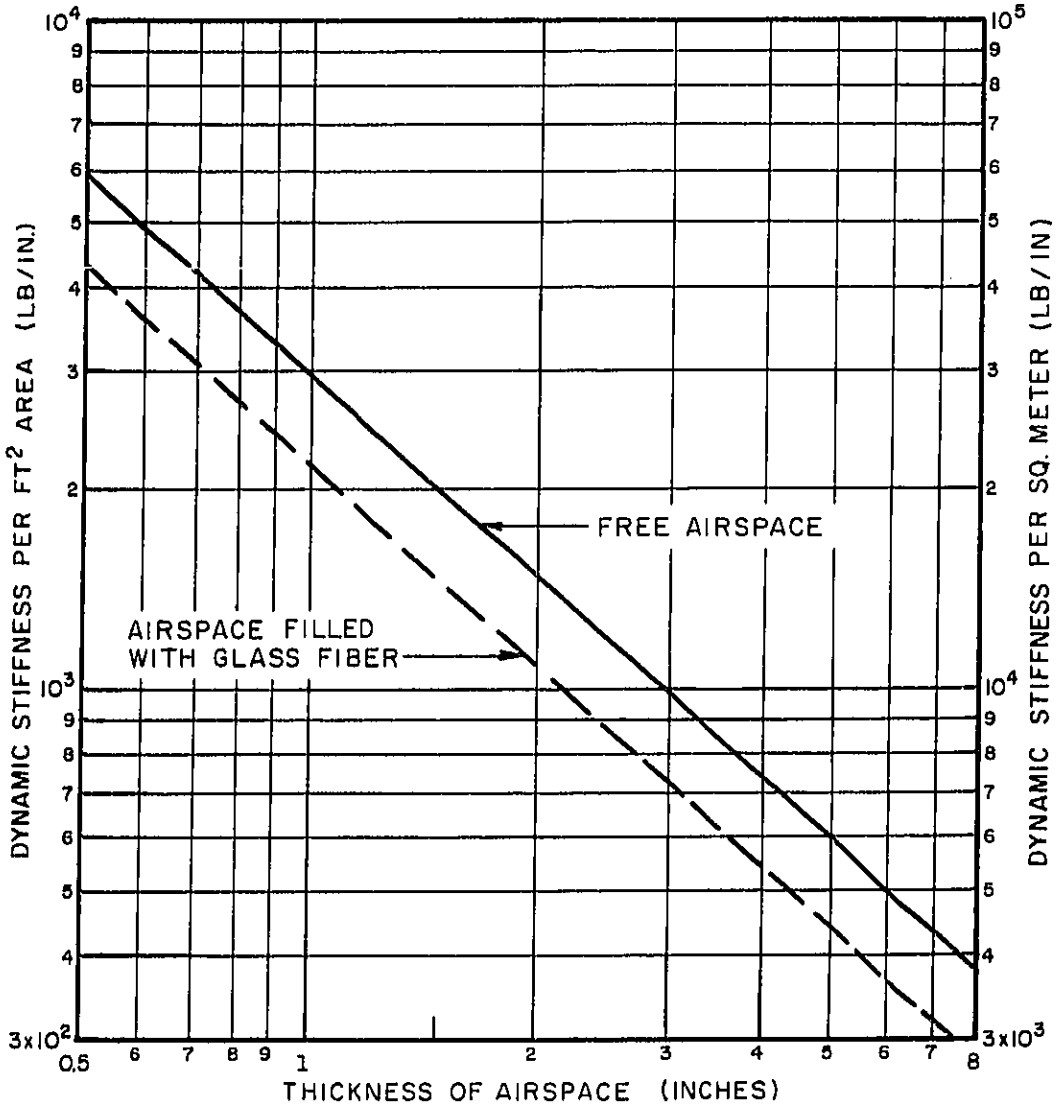

FIG. 2 DYNAMIC STIFFNESS VS AIRSPACE THICKNESS FOR AIR CUSHIONS OF UNIT AREA

air volume is larger than the stiffness of the mounts, the somewhat stiffer cork and neoprene mounts can perform nearly as well as a softer precompressed glass fiber mount. If the cork or neoprene provide better resistance against environmental factors, they can be used without substantial increase of the basic resonance frequency.

IV. HIGH FREQUENCY BEHAVIOR

A. Transmission of Vibration from the Floating Slab to the Structural Slab through a Mount

In dealing with the high frequency behavior of the floating slab system, we assume that the point admittance of the slabs for bending waves is like that of an infinite plate, i.e., real and independent of frequency. This assumption is certainly not valid at low frequencies for a single mount. But since very many mounts are involved in conducting vibrational energy between the two slabs, we shall assume that the average point input admittance over a finite plate can be approximated by the admittance of the infinite plate.

Using this assumption, we calculate the power transmitted through a mount of impedance Z from the floating slab (slab 1) to the structural slab (slab 2) when an incident bending wave of the velocity amplitude v_0 arrives at the mount. Sketch SK-2 shows the slab arrangement and defines the notations.

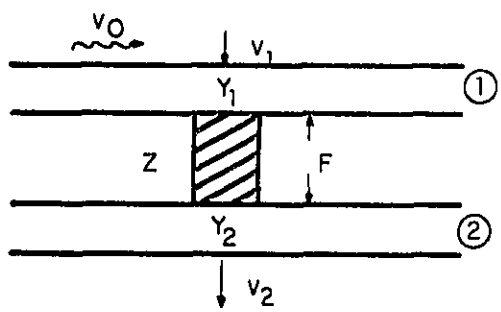

SK-2. Schematic slab arrangement.

v_0 = peak amplitude of the arriving bending wave, assumed simple harmonic

v_1 = peak normal velocity of slab 1 at the mount, assumed simple harmonic

v_2 = peak normal velocity of slab 2 at the mount, assumed simple harmonic

Y_1, Y_2 = point input admittance of the infinite slab, assumed real

Z = lumped impedance of the mount

F = peak dynamic force exerted on both slabs by the mount, assumed simple harmonic

The following three equations permit us to calculate the force and power transmitted from slab 1 to slab 2:

$$F = (v_1 - v_2)Z \tag{16a}$$

$$v_1 = v_0 - Y_1 F \tag{16b}$$

$$v_2 = Y_2 F \ . \tag{16c}$$

Solving the above equations for the force gives

$$F = v_0 \frac{Z}{1+Z(Y_1+Y_2)} \ . \tag{17}$$

In order to obtain F conjugate, F*, it is convenient to rewrite Eq. 17 in a form where its denominator is real:

$$F = v_0 \frac{Z+|Z|^2(Y_1+Y_2)}{1+(Z+Z^*)(Y_1+Y_2)+|Z|^2(Y_1+Y_2)^2} \tag{18}$$

and

$$F^* = v_0 \frac{Z^*+|Z|^2(Y_1+Y_2)}{1+(Z+Z^*)(Y_1+Y_2)+|Z|^2(Y_1+Y_2)^2} \ . \tag{19}$$

The asterisk as superscript indicates the complex conjugate of a symbol.

The power transmitted from slab 1 to slab 2 is given by

$$\pi_{12} = (1/2)\ \mathrm{Re}\{FF^*Y_2\} \ . \tag{20}$$

(Since the bending wavelength in the frequency region of interest is much smaller than the horizontal dimension of a typical floor mount, the power transfer through bending moment is negligible compared with the power transfer through the force.)

Following some elementary calculations, we obtain

$$\pi_{12} = \frac{v_0^2}{2} \frac{|Z|^2 Y_2}{1+(Z+Z^*)(Y_1+Y_2)+|Z|^2 (Y_1+Y_2)^2} , \qquad (21)$$

where π_{12} is the time average power and v_0 is the peak value of the transverse velocity in slab 1.

In the following statistical considerations we will be dealing with the space average of the slab velocity; therefore, we substitute $\langle v_0^2 \rangle_x$ for $v_0^2/2$ in Eq. 21 so that

$$\pi_{12} = \langle v_0^2 \rangle_x \frac{|Z|^2 Y_2}{1+(Z+Z^*)(Y_1+Y_2)+|Z|^2 (Y_1+Y_2)^2} = \langle v_0^2 \rangle_x K_{12}(\omega) , \qquad (22a)$$

giving

$$K_{12}(\omega) = \frac{|Z|^2 Y_2}{1+2\mathrm{Re}\{Z\}(Y_1+Y_2)+|Z|^2 (Y_1+Y_2)^2} . \qquad (22b)$$

B. Sound Transmission Loss of the Single Structural Slab

Since we are primarily interested in the increase in transmission loss, ΔTL, provided by the addition of the floating floor to the structural floor, the TL of the structural floor alone – as well as the TL of the composite structure – must be calculated. The calculation of the structural floor TL is less complicated, so we use it to provide insight into the statistical energy analysis procedure that will also be used for the TL calculation of the more complicated composite structure. To understand more clearly the physical phenomenon of the sound transmission, we distinguish

between the so-called forced (or mass-law) transmission and transmission by the resonant modes.

1. Forced transmission

If a sound wave strikes a partition at an oblique angle, the wall reacts to the sound wave by yielding to the local pressure. The forced wave in the wall, as a direct response to the exciting sound wave, propagates with the trace velocity of the sound wave, which for low frequencies is usually much greater than the propagation speed of free bending waves in the wall at the same frequency.

If we disregard for a moment the free bending waves that are always present in a resonant system of finite dimensions (due to reflections of the forced wave at the boundaries), we obtain a locally reacting mass-like behavior. The amplitude of the wall's transverse velocity at each point is proportional to the local pressure, and the transmission loss is given by the mass law:

$$TL(\theta) \approx 20 \log \frac{\rho_s \omega}{2\rho_0 c_0} \cos\theta \ , \qquad (23)$$

where ρ_s is the surface density of the wall and θ is the angle of incidence (normal incidence = 0°).[a]

From Eq. 23 we see that the TL is dependent on the angle of incidence. If one averages over all angles of incidence from θ=0° to θ=80°, one obtains the so-called field incidence TL:

$$TL_{field} \approx 10 \log \frac{1}{\pi} \left(\frac{\rho_s \omega}{2\rho_0 c_0} \right)^2 \qquad (24)$$

or

$$TL_{field} = 20 \log W_s + 20 \log f - 33 \text{ dB} \ , \qquad (25)$$

[a] The symbol 'log' refers to the 10-base logarithm throughout this report.

where W_s is the surface weight in lb/ft^2 and f is the frequency in Hz. Equation 25 is plotted in Fig. 3.

The field incidence TL given in Eq. 25 should be considered as an upper limit for the sound transmission loss (for nonabsorbing walls) that can be achieved only in the complete absence of the resonant waves.

Since the velocity of free bending waves is frequency dependent and at low frequencies (well below the critical frequency) is small compared with the velocity of sound in the surrounding medium, the free bending waves do not radiate efficiently in the low frequency range. Consequently, the TL is often successfully predicted by the mass law (Eq. 25).

2. Sound transmission by the resonant modes

In addition to the sound energy transmitted by the forced waves, free bending-wave resonances (excited by the forced wave) transmit an additional amount of sound energy and thus reduce the transmission loss of the wall. If we calculate the "mass-law transmission loss" and the "resonant mode transmission loss" separately, we can calculate the actual transmission loss on the basis of the total transmitted power. Should the "mass-law TL" be the same as the "resonant mode TL", the actual TL would then be 3 dB below the value calculated from the mass law alone.

First we describe qualitatively the process of sound transmission by these free resonant waves. As mentioned earlier, the bending wave speed depends on frequency, increasing with the square root of frequency. At low frequencies the bending wave speed is small compared with the velocity of sound; and the air acted upon by different parts of the plate vibrating in opposite phases can be shuffled back and forth without being compressed and, therefore,

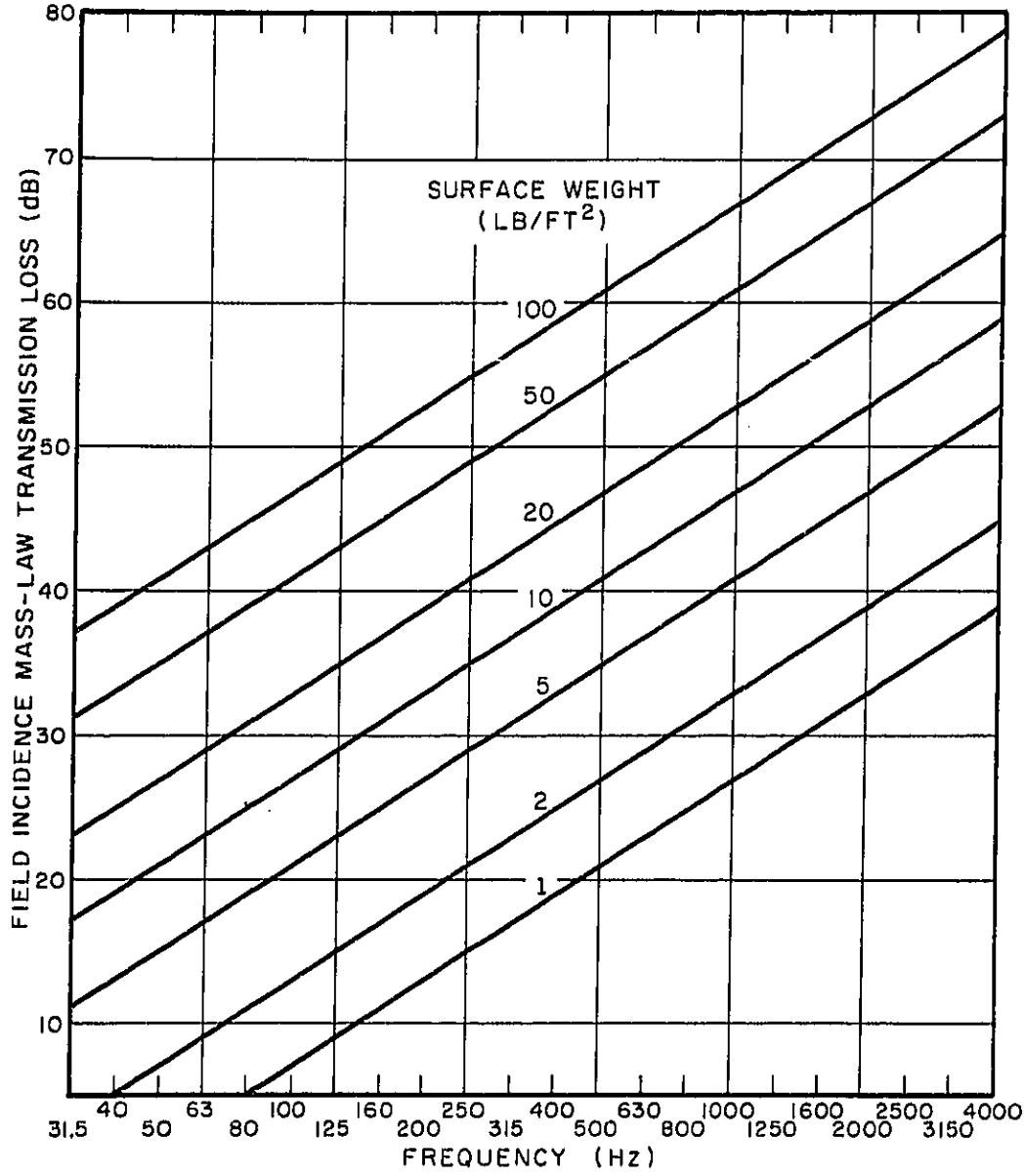

FIG. 3 FIELD INCIDENCE MASS-LAW TL VS FREQUENCY WITH THE PARTITIONS SURFACE WEIGHT AS PARAMETER

without causing effective sound radiation. Only at the edges and corners of the plate, where such a compensation is not possible and a net volume change occurs, will there be some sound radiation.

Near and above the coincidence frequency,[a] however, the bending wave speed has the same order of magnitude as the sound velocity. The free bending waves radiate efficiently from every point of the wall surface, and the sound transmission loss in this region is usually controlled by resonance rather than by forced waves. If the structure does not have sufficient structural damping, the free bending waves can run many times across the plate (radiating sound efficiently) without noticeable loss in amplitude; consequently, the TL in this region depends very much on the structural damping.

The qualitative discussion given above in terms of a wall is equally applicable to a floor slab.

The energy balance of the basic slab for resonant modes can be written as

$$\pi_{as} = \pi_{loss} + \pi_{rad} , \tag{26}$$

where π_{as} is the power flow from the acoustical field into the resonant modes of the structure, π_{loss} is the power lost in the structure due to internal damping and edge losses, and π_{rad} is the power loss due to acoustical radiation of the structure.

According to the statistical energy analysis [2], the above power balance can be written as

$$n_{as}\omega n_a\left[\frac{E_a}{n_a} - \frac{E_s}{n_s}\right] = E_s\omega\eta_s + \rho_0 c_0 A\sigma_{rad}\langle v^2\rangle , \tag{27}$$

where n_a = acoustical modal density in the source room
n_s = structural modal density in the structural slab

[a] The coincidence frequency of a homogeneous slab is given in Eq. 45.

E_a = total acoustical energy in the source room[a]

E_s = total mechanical energy in the structural slab

η_s = loss factor of the slab

A = slab surface area

σ_{rad} = radiation efficiency of the slab

η_{as} = coupling loss factor (from acoustic to structural slab)

$\langle v^2 \rangle$ = mean square slab velocity

ρ_0 = density of air

c_0 = velocity of sound in air.

Since η_{as} is not well known, we shall replace it by know quantities.

From $\pi_{as} = -\pi_{sa}$ it follows that

$$\left[\frac{E_a}{n_a} - \frac{E_s}{n_s}\right] n_a \omega \eta_{as} = -\left[\frac{E_s}{n_s} - \frac{E_a}{n_a}\right] n_s \omega \eta_{sa} \ , \qquad (28)$$

which gives

$$\eta_{as} = \frac{n_s}{n_a} \eta_{sa} \ . \qquad (29)$$

The definition of the loss factor is

$$\pi_{sa} = E_s \omega \eta_{sa} = \langle v^2 \rangle \rho_s A \omega \eta_{sa} = \langle v^2 \rangle \rho_0 c_0 A \sigma_{rad} \ , \qquad (30)$$

providing

---

[a] E_a and E_s are measured within a unit bandwidth centered at the frequency, ω.

$$\eta_{sa} = \frac{\rho_0 c_0}{\rho_s \omega} \sigma_{rad} \ , \tag{31}$$

where ρ_s is the surface mass density of the slab.

Putting Eqs. 29 and 31 into Eq. 27 gives

$$\left[\frac{E_a}{n_a} - \frac{E_s}{n_s}\right] n_s \frac{\rho_0 c_0}{\rho_s} \sigma_{rad} = E_s \omega \eta_s + \langle v^2 \rangle \rho_0 c_0 A \sigma_{rad} \ . \tag{32}$$

The acoustical and vibrational energy is

$$E_a = \frac{\langle p_1^2 \rangle}{\rho_0 c_0^2} V \tag{33}$$

and

$$E_s = \langle v^2 \rangle \rho_s A \ , \tag{34}$$

where $\langle p_1 \rangle^2$ is the mean square pressure in the source room and V is the volume of the source room. Thus, we obtain for the mean square slab velocity, as a function of the source room pressure,

$$\langle v^2 \rangle = \langle p_1^2 \rangle \frac{n_s}{n_a} \frac{V}{A} \frac{\sigma_{rad}}{c_0 \rho_s} \frac{1}{\rho_s \omega \eta_s + 2\rho_0 c_0 \sigma_{rad}} \ . \tag{35}$$

The power radiated by the slab into the receiving room is

$$\pi_{ac} = \rho_0 c_0 A \sigma_{rad} \langle v^2 \rangle \tag{36}$$

$$\pi_{ac} = \langle p_1 \rangle^2 \frac{n_s}{n_a} \frac{V}{A} \frac{\rho_0}{\rho_s} \frac{\sigma_{rad}^2 A}{\rho_s \omega \eta_s + 2\rho_0 c_0 \sigma_{rad}} \ . \tag{37}$$

The power incident on the slab from the source room is [3]

$$\pi_{in} = \frac{\langle p_1 \rangle^2}{4\rho_0 c_0} A \quad . \tag{38}$$

The ratio of the incident to transmitted acoustical power is consequently

$$\frac{\pi_{in}}{\pi_{ac}} = \frac{\frac{\langle p_1 \rangle^2}{4\rho_0 c_0} A}{\langle p_1 \rangle^2 \frac{n_s}{n_a} \frac{V}{A} \frac{\rho_0}{\rho_s} \frac{\sigma_{rad}^2}{c_0} \frac{A}{\rho_s \omega \eta + 2\rho_0 c_0 \sigma_{rad}}} \quad , \tag{39}$$

which simplifies to:

$$\frac{\pi_{in}}{\pi_{ac}} = \frac{1}{4\sigma_{rad}} \frac{\frac{\rho_s A}{n_s}}{\frac{\rho_0 V_0}{n_a}} \frac{\rho_s \omega \eta + 2\rho_0 c_0 \sigma_{rad}}{\rho_0 c_0 \sigma_{rad}} \tag{40}$$

or

$$TL = 10 \log \frac{1}{4\sigma_{rad}} \frac{\frac{m_s}{n_s}}{\frac{m_0}{n_a}} \frac{\eta_{tot}}{\eta_{ac}} \quad , \tag{41}$$

where m_s is the total mass of the slab and m_0 is the mass of the air in the source room.

The TL is directly proportional to the ratio of slab mass per structural mode to air mass in the source room per acoustical mode, and also proportional to the ratio of total loss factor to the

acoustical loss factor; the TL is inversely proportional to the radiation efficiency of the slab. If one replaces n_a and n_s with their actual numerical values, the TL naturally becomes independent of room volume and slab surface area. Equation 41 is easy to remember and provides a remarkably simple solution to a complicated problem.

In order to obtain the "resonant-TL" of the slab, we put [2]

$$n_a = \frac{4\pi f^3 V}{c_0^3} \tag{42}$$

and

$$n_s = \frac{\sqrt{12}\, A}{2 c_L h} \tag{43}$$

into Eq. 40 and obtain

$$\frac{\pi_{in}}{\pi_{ac}} = \frac{2\pi f^2 c_L h \rho_s}{\sqrt{12}\, c_0^3 \rho_0 \sigma_{rad}} \frac{n_{tot}}{n_{rad}} . \tag{44}$$

Using $(n_{tot}/n_{rad}) \approx (\rho_s \omega \eta)/(\rho_0 c_0 \sigma_{rad})$ and considering the equation for the coincidence frequency,[a]

$$f_c = \frac{\sqrt{12}}{2\pi} \frac{c_0^2}{h c_L} , \tag{45}$$

where h is the slab thickness, we get

---

[a] Figure 4 gives the coincidence frequency for dense and lightweight concrete slabs as a function of the slab thickness.

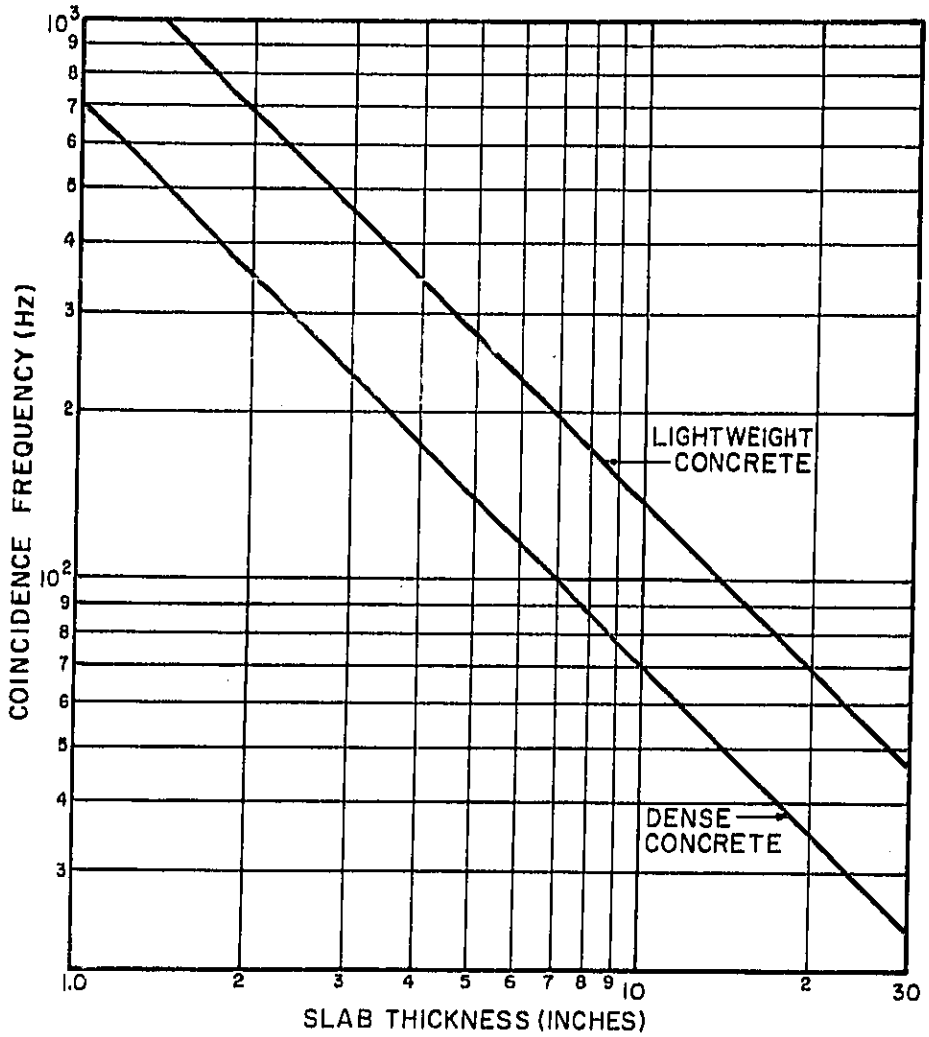

FIG. 4 COINCIDENCE FREQUENCY VS THICKNESS FOR HOMOGENEOUS CONCRETE PARTITIONS

$$\frac{\pi_{in}}{\pi_{ac}} = \frac{4\pi^2 \rho_s f^2}{\rho_0^2 c_0^2} \frac{f}{f_c} \frac{\eta}{\sigma_{rad}^2} = \frac{1}{\pi} \left[\frac{\rho_s \omega}{\rho_0 c_0}\right]^2 \frac{f}{f_c} \frac{2\eta}{\sigma_{rad}^2} \quad . \tag{46}$$

Recognizing that the first term in Eq. 46 is the field incidence transmission, the "resonant TL" can be written as

$$TL_{res} = TL_{field} + 10 \log \frac{f}{f_c} \cdot \frac{2\eta}{\sigma_{rad}^2} \quad . \tag{47}$$

When $[(f/fc)(2\eta/\sigma_{rad}^2)] < 1$, the "resonant TL" is smaller than the field incidence mass law TL.

Below the critical frequency and when the dimensions of the slab are large compared with the acoustical wavelength, the radiation efficiency σ_{rad} can be approximated [4] by the following function:

$$\sigma_{rad} = \frac{P_{rad}}{A} \frac{c_0}{f_c} g\left(\frac{f}{f_c}\right) \quad ; \quad f < f_c \quad , \tag{48}$$

where A is the surface area of the slab, P_{rad} is the radiating perimeter (which is the actual slab perimeter plus twice the length of all stiff ribs or flexible joints, if any). The function $20 \log [g(f/f_c)]$ is plotted in Fig. 5.

Above the critical frequency the radiation efficiency becomes unity and the TL for the resonant modes can be calculated according to Eq. 47:

$$TL_{res} = TL_{field} + 10 \log \frac{2f}{f_c} \eta \quad ; \quad f > f_c \quad . \tag{49}$$

Figure 6 shows the calculated resonant TL of Eq. 47 and the field incidence mass law TL of Eq. 24 for a 12-in.-thick 121 lb/ft^2 dense

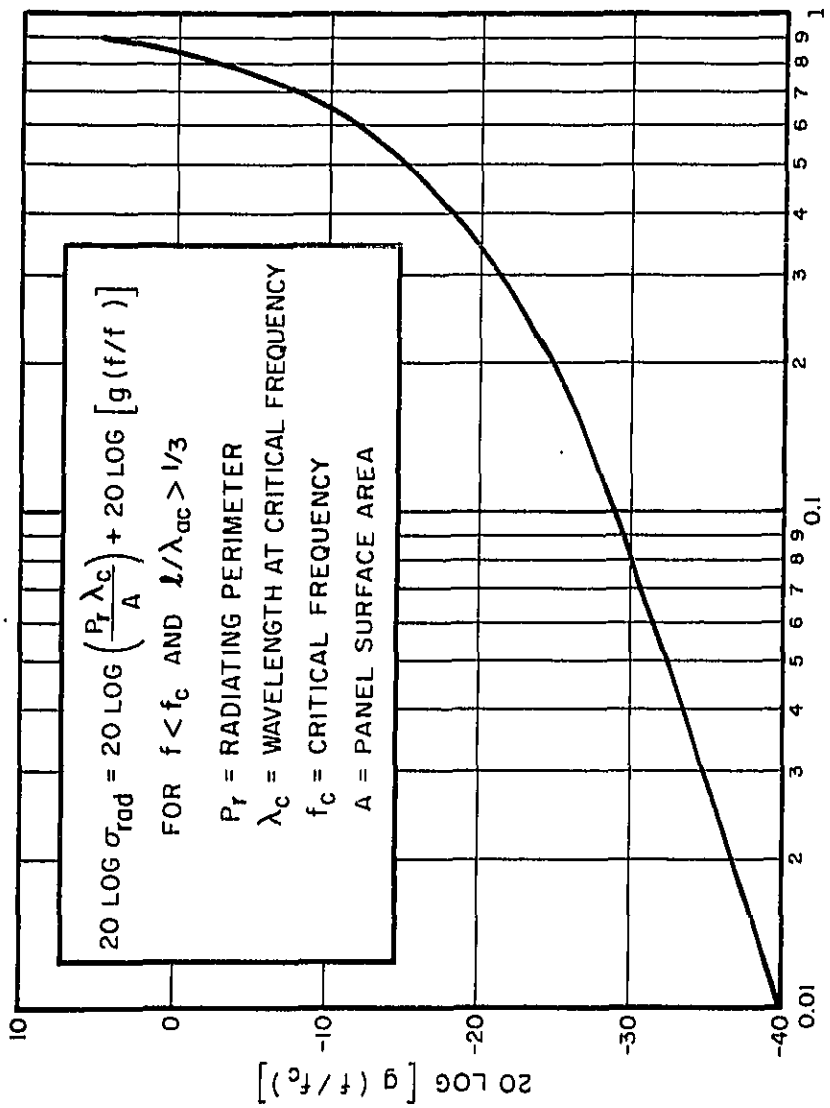

FIG. 5 20 LOG $\left[g\left(f/f_c\right)\right]$ VS NORMALIZED FREQUENCY f/f_c

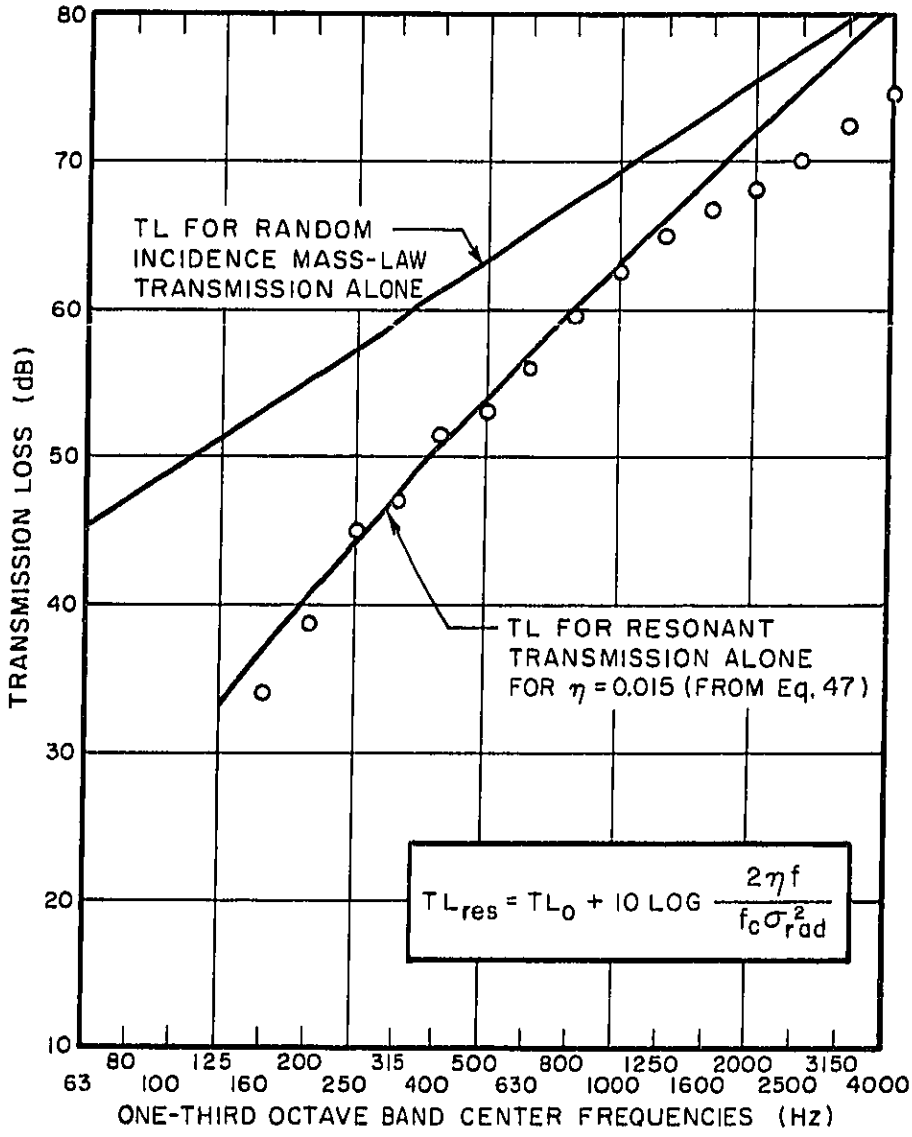

FIG. 6 TL VS FREQUENCY CURVE FOR A 12" THICK DENSE CONCRETE PARTITION
o MEASURED
—— CALCULATED

concrete block wall. The circles show the measured values obtained in a laboratory test.[a] The loss factor (η=0.015) represents the viscous losses plus the power loss through conduction of vibrational energy into adjoining structural elements. The agreement between the measured and calculated TL is very good.

C. Sound Transmission Loss of the Composite Floor

1. Forced wave transmission

The sound waves incident on a floating slab force it to respond locally to the sound pressure. In the absence of the vibration isolating mount and the structural slab, the forced response of the (infinite) floating slab would obey the mass law.

The presence of the vibration isolator creates a force which resists the motion of the floating slab; and this resisting force is transmitted through the isolator to the structural slab, forcing it to respond. Since the forced excitation runs along the floating slab with the trace velocity of the incoming waves, the forced response of the structural slab is an effective radiator with a radiation efficiency of nearly unity.

The sound pressure of the incoming sound wave p_1 must be balanced by both the inertial force of the floating slab and the restoring force of the isolator:

$$p_1 = i\rho_{s_1}\omega v_1 + n'Zv_1 \qquad (50)$$

where ρ_{s_1} is the surface mass density of the floating slab, v_1 is

[a] National Gypsum Company, 14 June 1967, Test No. 3002.

its velocity at the isolator, Z is the impedance of the isolator and n' is the number of isolators per unit area. The force transmitted to the structural slab through each isolator is given by

$$F \approx Zv_1 \qquad \text{for} \quad v_1 >> v_2 \quad . \tag{51}$$

Using the value of v_1 from Eq. 40, we get

$$F = Zv_1 = \frac{Z}{i\rho_{s_1}\omega + n'Z}\, p_1 \quad . \tag{52}$$

The forced mass law response of the structural slab is

$$v_2 = \frac{Fn'}{i\rho_{s_2}\omega} \quad , \tag{53}$$

where ρ_{s_2} is the surface mass density of the structural slab. The sound power radiated by the structural slab is

$$\pi_{2a_F} = v_2^2\, \rho_0 c_0 A = - \frac{n'}{\rho_{s_1}^2 \omega^2} \left| \frac{Z}{i\rho_{s_1}\omega + n'Z} \right|^2 \langle p_1^2 \rangle \rho_0 c_0 A \quad . \tag{54}$$

Assuming the mount is adequately represented by a spring with viscous damping, we get

$$Z = - i \frac{k}{\omega} + r \quad , \tag{55}$$

where r represents the real part of the impedance of the mount. The power incident on the floating slab from the source room is

$$\pi_{1a} = \frac{\langle p_1^2 \rangle}{4\rho_0 c_0} A \tag{56}$$

$$\frac{\pi_{1a}}{\pi_{2a_F}} = \frac{\omega^2 \rho_{s_2}^2}{4n'^2(\rho_0 c_0)^2 \left| \frac{Z}{i\rho_{s_1}\omega + n'Z} \right|^2} . \qquad (57)$$

Using Eq. 55 and making the justified assumption that $k/\omega > r$, we obtain the following approximations for the forced wave transmission loss: above the natural frequency where $\rho_{s_1}\omega > (k/\omega)n'$,

$$TL_F = 10 \log \frac{\rho_{s_1}^2 \rho_{s_2}^2 \omega^6}{4n'^2 k^2 (\rho_0 c_0)^2} ; \qquad (58)$$

at the natural frequency of the floor where $n'(k/\omega) = \rho_{s_1}\omega$,

$$TL_F = 10 \log \frac{\rho_{s_2}^2 r^2 \omega_0^4}{4k^2(\rho_0 c_0)^2} = 10 \log \frac{\rho_{s_2}^2 r^2 n'^2}{4\rho_{s_1}^2 (\rho_0 c_0)^2} . \qquad (59)$$

Equation 58 gives the forced-wave TL_F of the composite floor above the natural frequency of the floor.

Equation 59 permits us to approximate the TL_F of the composite floor at the resonance frequency of the floor.

2. Resonant transmission

The power supplied to the floating slab by the acoustical field is partly transmitted through the isolators to the structural slab, partly dissipated in the floating slab itself, and partly reradiated as sound toward the source room. A part of the power transmitted through a mount into the structural slab will re-enter the floating slab through the other mounts.

The power balance reads

$$\pi_{as} = \pi_{12} + \pi_{\eta_1} + \pi_{rad_1} - \pi_{21} \tag{60}$$

where π_{as} = power introduced into the floating slab by the acoustical field

π_{12} = power transmitted from the floating slab to the structural slab through the isolators

π_{rad_1} = acoustical power radiated by the floating slab

π_{η_1} = power lost in the floating slab due to its internal damping

π_{21} = power transmitted from the structural slab back into the floating slab.

Using the same nomenclature as for the single slab calculations in Sec. IV.B.2, and recalling the value of π_{12} from Eq. 22,

$$\pi_{12} = \langle v_1^2 \rangle K_{12}(\omega) n' A = \langle v_j^2 \rangle \frac{n' A \, |Z|^2 Y_2}{1+(Z+Z^*)(Y_1+Y_2)+|Z|^2 (Y_1+Y_2)^2} , \tag{61}$$

we can write the power balance as:

$$\pi_{as} = \eta_{as} \omega n_a \left[\frac{E_a}{n_a} - \frac{E_{s_1}}{n_{s_1}}\right] = \langle v_1^2 \rangle A \left[K_{12}(\omega) n' + \rho_{s_1} \omega \eta_1 + \rho_0 c_0 \sigma_{rad_1}\right]$$

$$- \langle v_2^2 \rangle K_{21}(\omega) n' A \tag{62}$$

where $K_{21}(\omega)$ can be immediately evaluated by changing the subscripts

in Eq. 22. Accordingly, we get:

$$K_{21}(\omega) = \frac{|Z|^2 Y_1}{1+(Z+Z^*)(Y_1+Y_2)+|Z|^2 (Y_1+Y_2)^2} = \frac{Y_1}{Y_2} K_{12}(\omega) \quad . \tag{63}$$

Combining Eqs. 29 and 31 gives

$$\eta_{as} = \frac{n_{s_1}}{n_a} \frac{\rho_0 c_0}{\rho_{s_1} \omega} \sigma_{rad_1} \quad . \tag{64}$$

Using Eqs. 33, 34, and 63, we get

$$\langle p_1^2 \rangle \frac{n_{s_1}}{n_a} \frac{\sigma_{rad_1}}{\rho_{s_1} c_0} V = \langle v_1^2 \rangle A \left[K_{12}(\omega) n' + \rho_{s_1} \omega \eta_1 + 2\rho_0 c_0 \sigma_{rad_1} \right]$$

$$- \langle v_2^2 \rangle \frac{Y_1}{Y_2} K_{12}(\omega) n' A \quad . \tag{65}$$

The power balance of the structural slab (slab 2) provides $\langle v_2^2 \rangle$ as a function of $\langle v_1^2 \rangle$. The power balance is

$$\pi_{12} = \pi_{\eta_2} + \pi_{rad_2} + \pi_{21} \quad , \tag{66}$$

where π_{η_2} is the power lost in the floating slab due to its internal damping and transmission of vibrational energy into adjoining structures.

Inserting the appropriate terms into Eq. 66, we get

$$\langle v_1^2 \rangle K_{12}(\omega) n' A = \langle v_2^2 \rangle A \left[\rho_{s_2} \omega \eta_2 + \rho_0 c_0 \sigma_{rad_2} + \frac{Y_1}{Y_2} K_{12}(\omega) n' \right] \quad , \tag{67}$$

which yields

$$\langle v_2^2 \rangle = \langle v_1^2 \rangle \frac{K_{12}(\omega)n'}{\rho_{s_2}\omega\eta_1+\rho_0 c_0 \sigma_{rad_2} + \frac{Y_1}{Y_2} K_{12}(\omega)n'} \quad . \tag{68}$$

Putting this value of $\langle v_2^2 \rangle$ into Eq. 65 and solving for $\langle v_1^2 \rangle$ gives

$$\langle v_1^2 \rangle = \frac{\langle p_1^2 \rangle \frac{n_{s_1}}{n_a} \frac{\sigma_{rad_1}}{\rho_{s_1} c_0} \frac{V}{A}}{K_{12}(\omega)n'+\rho_{s_1}\omega\eta_1+2\rho_0 c_0 \sigma_{rad_1} - \frac{\frac{Y_1}{Y_2}[K_{12}(\omega)n']^2}{\rho_{s_2}\omega\eta_2+\rho_0 c_0 \sigma_{rad_2}+\frac{Y_1}{Y_2} K_{12}(\omega)n'}} \tag{69}$$

Combining Eqs. 68 and 69 yields the velocity of the structural slab:

$$\langle v_2^2 \rangle = \frac{\langle p_1^2 \rangle \frac{V}{A} \frac{n_{s_1}}{n_a} \frac{\sigma_{rad_1}}{\rho_{s_1} c_0} \frac{K_{12}(\omega)n'}{\rho_{s_2}\omega\eta_2+\rho_0 c_0 \sigma_{rad_2} + \frac{Y_1}{Y_2} K_{12}(\omega)n'}}{K_{12}(\omega)n'+\rho_{s_1}\omega\eta_1 + 2\rho_0 c_0 \sigma_{rad_1} - \frac{\frac{Y_1}{Y_2}[K_{12}(\omega)n']^2}{\rho_{s_2}\omega\eta_2+\rho_0 c_0 \sigma_{rad_2}+\frac{Y_2}{Y_1} K_{12}(\omega)n'}} \tag{70}$$

The acoustic power radiated by the resonant bending waves of the structural slab is:

$$\pi_{2a_R} = \langle v_2^2 \rangle \rho_0 c_0 \sigma_{rad_2} A \quad . \tag{71}$$

Now considering that for thick concrete walls the radiation term ($\rho_0 c_0 \sigma_{rad}$) is always small compared with the internal loss terms ($\rho_s \omega \eta$) and inserting Eq. 70 into Eq. 71 we get:

$$\pi_{2a_R} = \frac{\langle p_1^2 \rangle \frac{V}{A} A \frac{\eta_{s_1}}{n_a} \frac{\rho_0}{\rho_{s_1}} \sigma_{rad_1} \sigma_{rad_2}}{\rho_{s_2} \omega \eta_2 \left[1 + \frac{\rho_{s_1} \omega \eta_1}{K_{12}(\omega) n'} + \frac{\rho_{s_1}}{\rho_{s_2}} \frac{\eta_1}{\eta_2} \frac{Y_1}{Y_2} \right]} \quad . \tag{72}$$

A qualitative evaluation of Eq. 72 reveals that above a certain frequency [defined by $\rho_{s_1} \omega \eta_1 = K_{12}(\omega) n'$][a] the acoustical power transmitted by the floating slab system decreases with the seventh power of the frequency. Furthermore, the transmitted power is indirectly proportional to the loss factor of the slabs and directly proportional to their radiation efficiency. Accordingly, the sound transmission loss of a floating slab system depends to a very large degree on the loss factor of the floating slab.

The acoustical power incident on the floating slab from the source room side is:

$$\pi_{in} = \frac{\langle p_1^2 \rangle}{4 \rho_0 c_0} A \quad . \tag{73}$$

---

[a] Since the floating slab does not have rigid connections with the rest of the structure, its loss factor, η_1, is governed by the viscous losses alone.

The logarithmic ratio of incident to transmitted power gives the sound transmission loss of the composite floor,

$$TL_{COMP_F} = 10 \log \frac{\pi_0}{\pi_{2a_F} + \pi_{2a_R}} , \qquad (74)$$

where the power transmitted by the forced waves, π_{2a_F}, and the power transmitted by the resonant waves, π_{2a_R}, are given in Eqs. 54 and 72, respectively. Using the above equations and replacing n_{s_1} n_a with their respective values from Eqs. 42 and 43, we obtain the sound transmission loss of the composite floor:

$$TL_{COMP} = 10 \log \left[\frac{1}{\left(\frac{2\rho_0 c_0 n' k}{\rho_{s_1} \rho_{s_2} \omega^3} \right)^2 + \frac{2\sqrt{12}\,(\rho_0 c_0)^2 c_0^2 \sigma_{rad_1} \sigma_{rad_2}}{c_L h_1 \rho_{s_1} \rho_{s_2} \eta_2 \omega^3 \left(1 + \frac{\rho_{s_1}}{\rho_s} \frac{Y_1}{Y_2} \frac{\eta_1}{\eta_2} + \frac{\rho_{s_1} \omega \eta_1}{K_{12}(\omega) n'} \right)}} \right] \qquad (75)$$

We are also concerned with the difference in sound transmission loss, ΔTL, between the composite and the single slabs. ΔTL is the logarithmic ratio of the total acoustic power transmitted by the single slab and the total acoustic power transmitted by the composite slab, namely:

$$\Delta TL = 10 \log \left[\frac{\left(\pi_{2a_F} + \pi_{2a_R} \right)_{single}}{\left(\pi_{2a_F} + \pi_{2a_R} \right)_{composite}} \right] . \qquad (76)$$

The transmitted powers are given in Eqs. 24, 37, 54, and 72, respectively. Inserting these in Eq. 76 gives:

$$\Delta TL = 10 \log \left[\frac{\left(\frac{\sqrt{\pi}}{\rho_{s_2} \omega} \right)^2 + \frac{\pi \sqrt{12}\, c_0^2 \sigma_{rad_2}^2}{2 c_{L_2} h_2 \rho_{s_2}^2 \eta_2 \omega^3}}{\left(\frac{n'k}{\rho_{s_1} \rho_{s_2} \omega^3} \right)^2 + \frac{\pi \sqrt{12}\, c_0^2 \sigma_{rad_1} \sigma_{rad_2}}{2 c_{L_1} h_1 \rho_{s_1} \rho_{s_2} \eta_2 \omega^3} \left(1 + \frac{\rho_{s_1}}{\rho_s} \frac{Y_1}{Y_2} \frac{\eta_1}{\eta_2} + \frac{\rho_{s_1} \omega \eta_1}{K_{12}(\omega) n'} \right)^{-1}} \right] \quad (77)$$

Assuming that the forced terms are negligible compared with the resonant terms, we can reduce Eq. 77 to

$$\Delta TL \approx 10 \log \left[\frac{h_1}{h_2} \frac{\rho_{s_1}}{\rho_{s_2}} \frac{c_{L_1}}{c_{L_2}} \left(1 + \frac{\rho_{s_1}}{\rho_{s_2}} \frac{Y_1}{Y_2} \frac{\eta_1}{\eta_2} + \frac{\rho_{s_1} \omega \eta_1}{K_{12}(\omega) n'} \right) \right] . \quad (78)$$

If both slabs are of the same material, then

$$\frac{\rho_{s_1}}{\rho_{s_2}} = \frac{h_1}{h_2} \quad ; \quad \frac{Y_1}{Y_2} = \frac{h_2^2}{h_1^2} \quad \text{and} \quad c_{L_1} = c_{L_2} .$$

Accordingly, for a common slab material the improvement in sound transmission loss is simply

$$\Delta TL \approx 10 \log \left[\frac{h_1^2}{h_2^2} \left(1 + \frac{h_2}{h_1} \frac{\eta_1}{\eta_2} + \frac{\rho_{s_1} \omega \eta_1}{K_{12}(\omega) \pi^2} \right) \right] . \qquad (79)$$

As we will prove later, $K_{12}(\omega)$ is proportional ω^{-2}. Consequently, above a certain frequency (above which the third sum in the bracket of the right side of Eq. 79 becomes larger than unity), ΔTL starts to increase with a slope of 30 dB per decade.

In order to evaluate our end results (Eqs. 77, 78, and 79), we had to measure the dynamic stiffness of the frequently used vibration isolation mountings as a function of static load. The measurement method and the measured dynamic stiffness and loss factor are reported in Sec. V.

V. MEASUREMENT OF THE DYNAMIC STIFFNESS AND LOSS FACTOR OF VARIOUS VIBRATION ISOLATION MOUNTS

The design of a floating floor or any other vibration isolation system requires knowledge of both the dynamic stiffness of the vibration isolation mounts (usually as a function of the static load and frequency) and the loss factor of the mounts. However, vibration isolator manufacturers almost never provide this important design information to their clients. Many times the only information given is the recommended loading and some type of an isolation factor. Occasionally, a load-deflection curve is provided; but though this might be sufficient for static design, it reveals little information about the dynamic properties needed for designing a vibration isolation system.

The purpose of the following experimental program was to measure the dynamic stiffness of a number of vibration isolation mounts currently used in floating floor construction.

A. Measurement Method

The measurement setup is shown in Fig. 7. The vibration isolator (sample) rests on a flat rigid foundation. The dynamic force is provided by an electrodynamic shaker and is applied to the sample through an impedance head (Wilcoxon Model Z6021) and an adapter. A static load is applied to the test sample at the adapter by the weights attached to the flexible piano wire. The impedance head provides two electric signals, one of which is proportional to the force acting across the impedance head, and the other, proportional to its acceleration.

The dynamic force F (which we would like to keep constant), acting on the sample, is smaller than the force measured by the

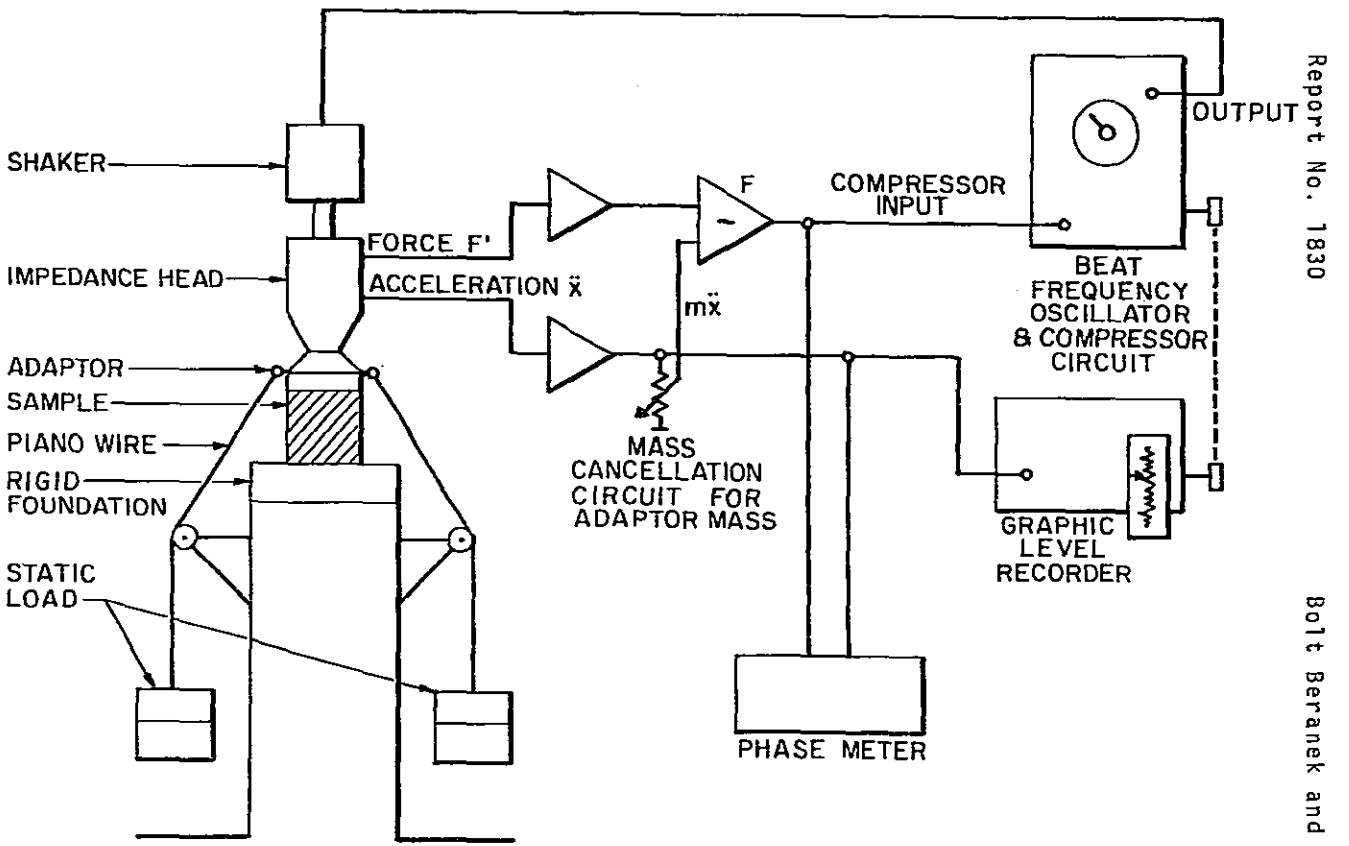

FIG. 7 SETUP FOR THE MEASUREMENT OF THE DYNAMIC STIFFNESS AND LOSS FACTOR

force gauge impedance head by the inertial force due to the adapter. In order to keep the dynamic force acting upon the sample constant, the shaker must supply the force,

$$F' = F + \ddot{x}m \ , \tag{80}$$

where m is the mass of the adapter, $\ddot{x}$ the acceleration of the adapter, and F the dynamic force acting on the sample. An electric signal proportional to $\ddot{x}m$ can be obtained by taking an appropriate fraction of the acceleration signal from the impedance head, as shown schematically in Fig. 7. By the addition of this term to the force signal, the inertia of the adapter mass is compensated — a process often referred to as electronic "mass cancellation".

In the present measurements it was possible to reduce the virtual mass of the adapter (the sample holder) to one-thirtieth of its actual value in the frequency range from 20 Hz to 4000 Hz. Above 4000 Hz, cancellation is not possible because of the first bending wave resonance of the sample holder.

Using electronic "mass cancellation", we could hold constant the dynamic force F acting upon the sample during each frequency sweep. A Bruel & Kjaer beat frequency oscillator supplied the excitation signal to the shaker and drove a Graphic Level Recorder, which recorded the acceleration signal as a function of frequency.

B. Measurement of the Dynamic Stiffness

The dynamic stiffness of the sample is defined as

$$k = \frac{F}{x} = \frac{F}{\left(\frac{-\ddot{x}}{\omega^2}\right)} = -\frac{\omega^2 F}{\ddot{x}} \tag{81}$$

and

$$|\ddot{x}| = \omega^2 \frac{F}{k} , \qquad (82)$$

where x is the displacement and k is the dynamic stiffness of the mount.

Since the dynamic force acting on the sample is held constant, the acceleration signal will increase with the square of the frequency if the dynamic stiffness of the mount is frequency independent. On a logarithmic plot of acceleration, the curve of acceleration vs frequency would then have a positive 40 dB per decade slope below the frequency of the lowest resonance that is due to the stiffness of the mount and the uncancelled mass of the adapter.

Figure 8 shows a typical acceleration vs frequency curve, obtained for a low-density cork mount in the form of a 2-in. cube. The acceleration response curve has a 40 dB/decade slope, indicating that the dynamic stiffness of the mount is independent of frequency. The first resonance frequency is around 1000 Hz. For comparison, the acceleration response for a pure mass is also shown in Fig. 8. For a constant force, the representation of this response is naturally a horizontal line. Actually, the response of the system to a known mass is used to evaluate the dynamic stiffness of the mount. Namely, at the frequency f*, where the horizontal line for the mass alone crosses the straight sloping part of the response of the mount, both mechanical impedances are equal:

$$kx = m\ddot{x} = -4\pi^2 f^{*2} mx , \qquad (83a)$$

and

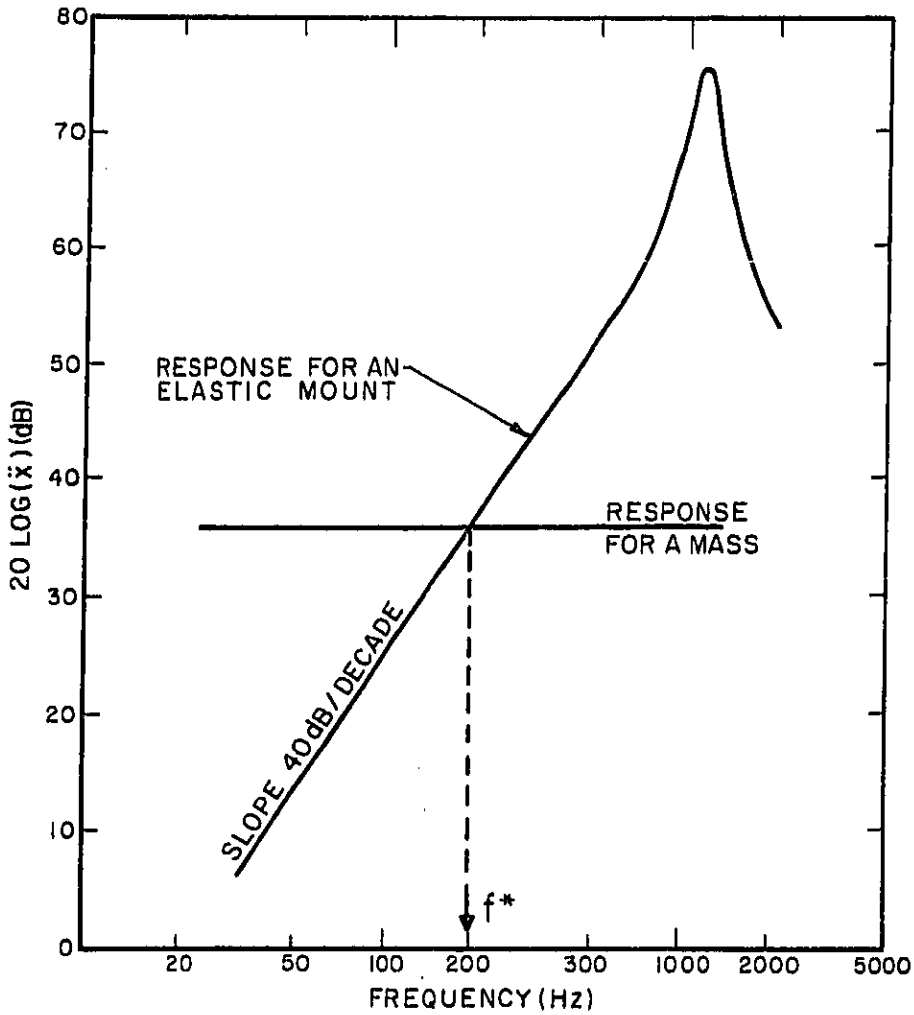

FIG. 8 TYPICAL ACCELERATION RESPONSE OF A VIBRATION ISOLATION MOUNT

$$k = 4\pi^2 f^{*2} m \ . \qquad (83b)$$

Both the frequency and the mass can be measured accurately.

C. Loss Factor Measurement

Let us assume a complex Young's modulus for the mount in the form:

$$\hat{E} = E\ (1+j\eta) \qquad (84)$$

where E is the real part of the Young's modulus and η is the loss factor. This gives the following relationship between dynamic force and acceleration:

$$F = -\frac{\ddot{x}k}{\omega^2}\ [1+j\eta] \ . \qquad (85)$$

Accordingly, the loss factor can be measured directly in terms of the angular phase difference α between the force and acceleration signals:

$$\eta = \tan \alpha \ . \qquad (86)$$

This method of measuring the loss factor is conceptually simple. In practice, however, even small disturbances — such as building vibration superimposed on one of the signals — make an accurate reading of the phase difference difficult at low signal levels. Such disturbances can be reduced by simultaneous filtering of both signals, provided that both filter sets have identical phase characteristics.

D. Dependence of the Dynamic Stiffness on Static Load

It is frequently observed that the dynamic stiffness of a vibration isolation mount increases with increasing static load. In designing a vibration isolation system, therefore, it is of prime importance to know the magnitude of the dynamic stiffness corresponding to the design static load.

The dependence of the dynamic stiffness of the sample mounts on static load was determined by recording the acceleration responses for various static loads applied to the sample. The apparatus used to record these responses is shown schematically in Fig. 7; the static load on the sample is given by vector addition of the tension forces in the loading wires.

Figure 9 shows the effect of the static load on the acceleration response for a 2-in. cube of standard density cork. The upper curve was obtained for no static load, the lower curve for 73-lb static load. It is clear from the Figure that the static load increases the dynamic stiffness by about 3 dB, corresponding to a 41% increase of the dynamic stiffness (that is, there is less acceleration for the same force excitation).

The stiffening effect of static load for a precompressed glass-fiber sample is much more pronounced. Figure 10 shows the acceleration response (for constant dynamic force) for a 2-in. cube of precompressed glass-fiber mount, both with and without static loading. The 73-lb static load increased the dynamic stiffness of this particular mount by 355%.

The dependence of the dynamic stiffness on static loading was evaluated for a number of vibration isolation mounts. Figures 11 and 12 summarize the results of these tests. The dynamic stiffness increased with increasing static load in all cases, but more so for the soft pads, such as the precompressed glass-fiber and

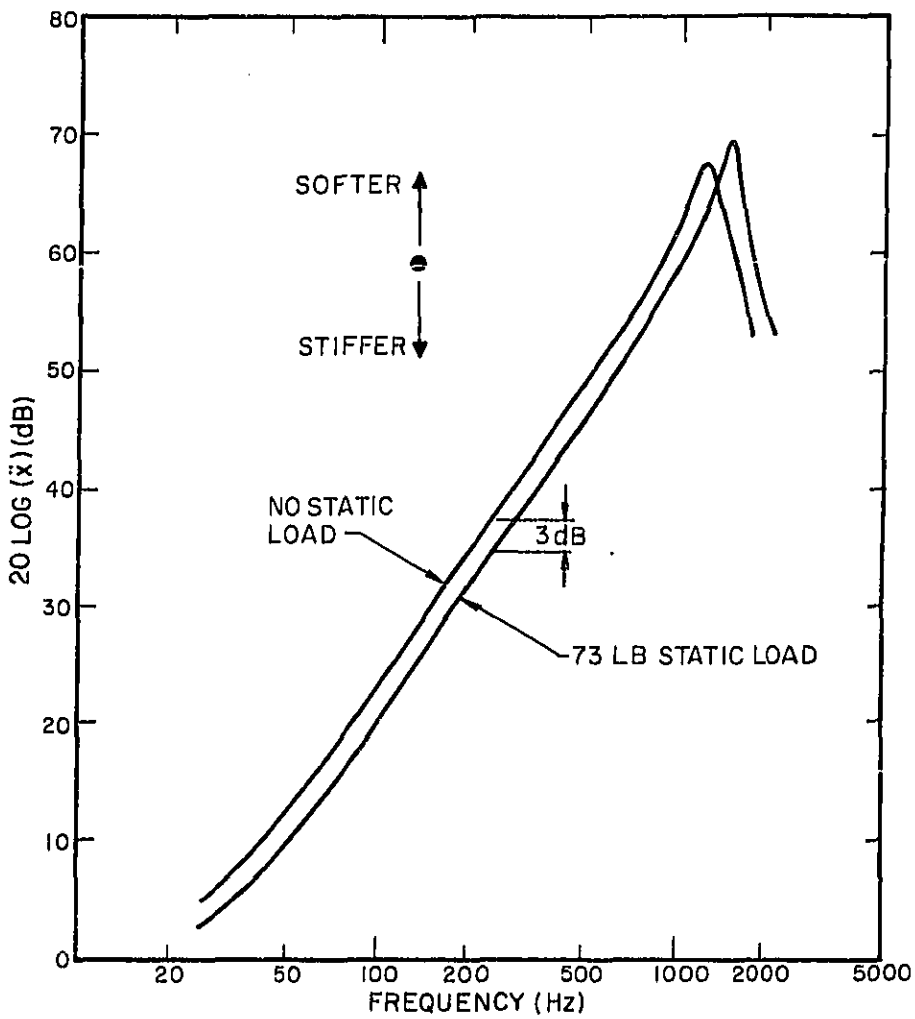

FIG. 9 STIFFENING EFFECT OF A STATIC LOAD ON A STANDARD DENSITY CORK MOUNT OF 2"x2"x2

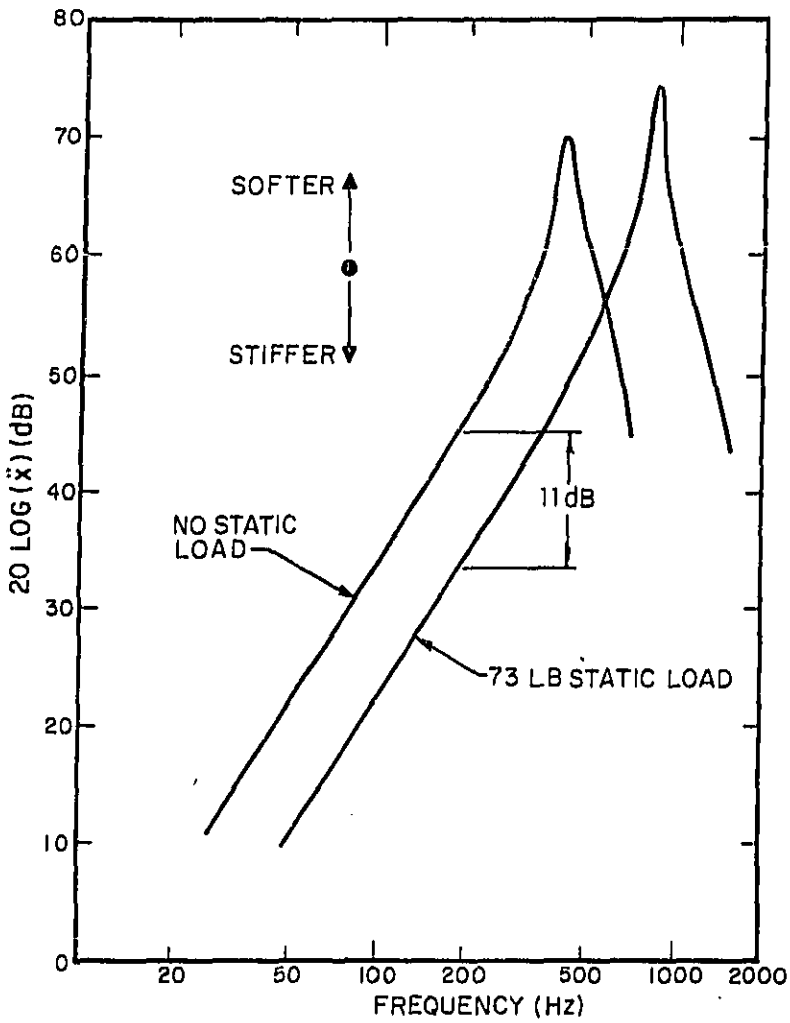

FIG. 10 STIFFENING EFFECT OF A STATIC LOAD ON A PRECOMPRESSED GLASS FIBER MOUNT OF 2"x2"x2"

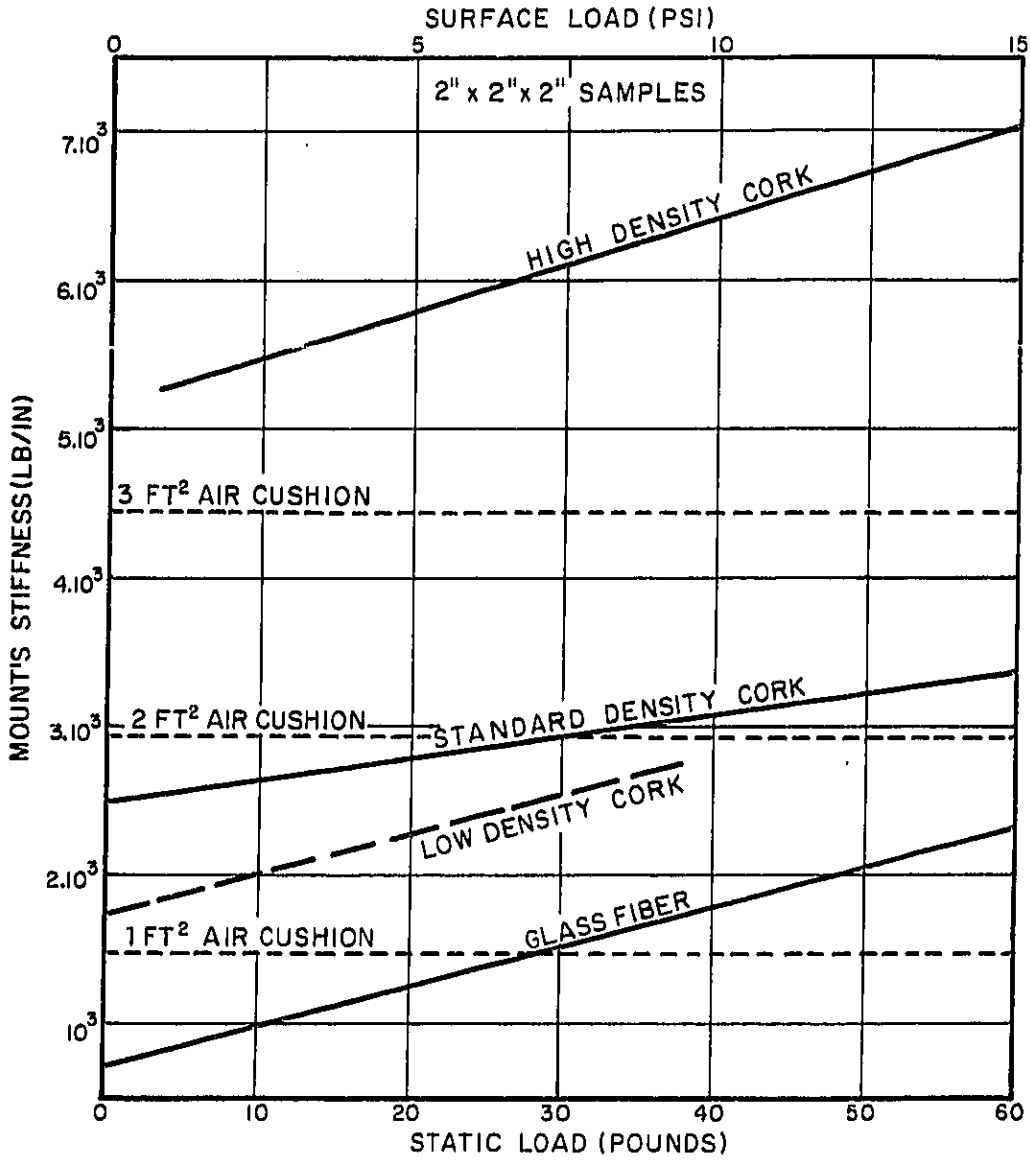

FIG. 11 MOUNT STIFFNESS VS STATIC LOAD FOR DIFFERENT 2"x2"x2" VIBRATION ISOLATION MOUNTS

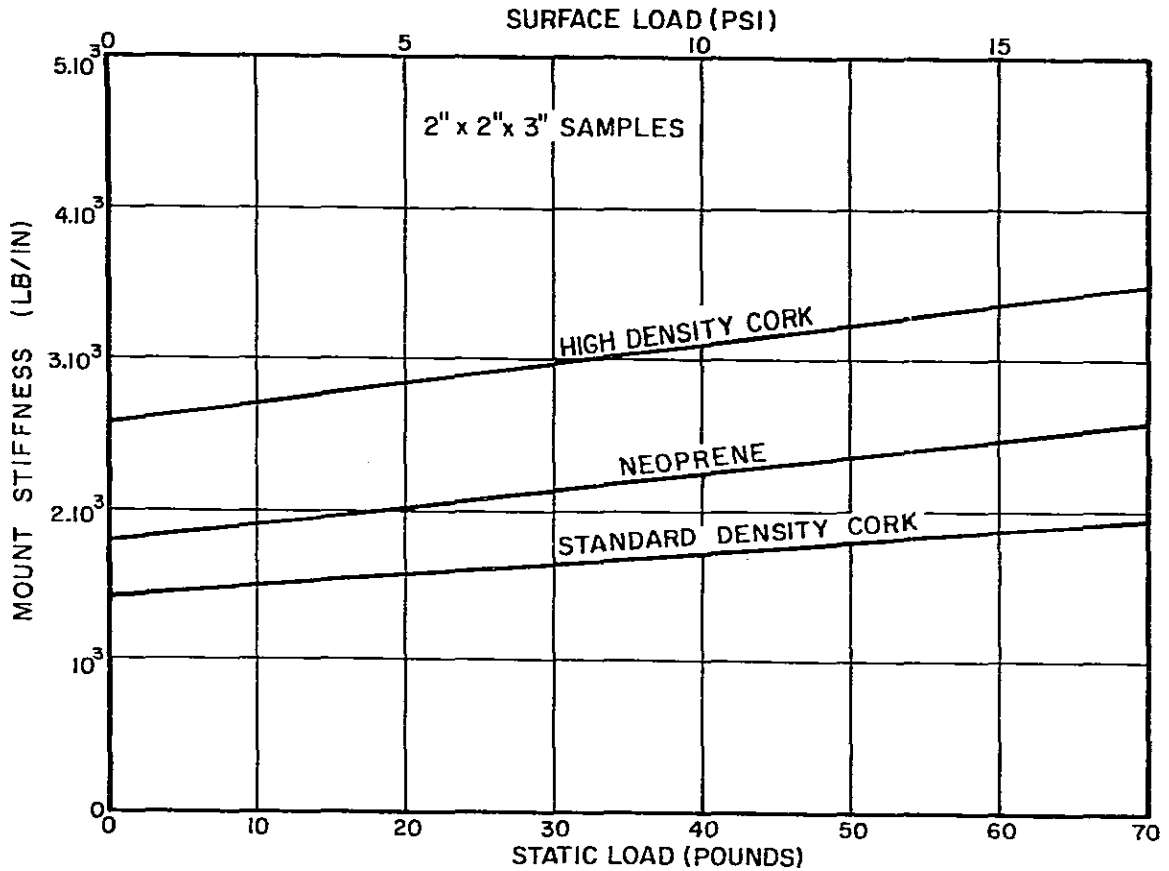

FIG. 12 MOUNT STIFFNESS VS STATIC LOAD FOR DIFFERENT 2" x 2" x 3" VIBRATION ISOLATION MOUNTS

light-density cork mount. In Figure 11 the dynamic stiffness of the enclosed air cushion is shown for comparison.

E. Resonance Method

In order to evaluate the dynamic stiffness of the vibration isolation mounts by a second independent method, the shaker, impedance head, and adapter assembly were inverted (turned 180°); the sample was then placed on the adapter and loaded with different known masses. The acceleration vs frequency curves obtained under these conditions for different mass loadings of the sample are shown in Fig. 13. At each resonance frequency, the inertia and stiffness terms cancel each other and the response is controlled by the resistive component of the impedance of the mount. Equating the inertia and stiffness terms yields the stiffness directly:

$$k = 4\pi^2 f_0^2 M = \omega_0^2 M \ , \tag{87}$$

where f_0 is the resonance frequency and M the added mass.

The nonresonant response at frequency ω_0 (obtained without the additional mass) is given by Eq. 82 as

$$|\ddot{x}| = \omega_0^2 \frac{F}{k} \ . \tag{88}$$

According to Eq. 85, the acceleration response with the added mass M is

$$|\ddot{x}_{res}| = \omega_0^2 \frac{F}{k\eta} \ , \tag{89}$$

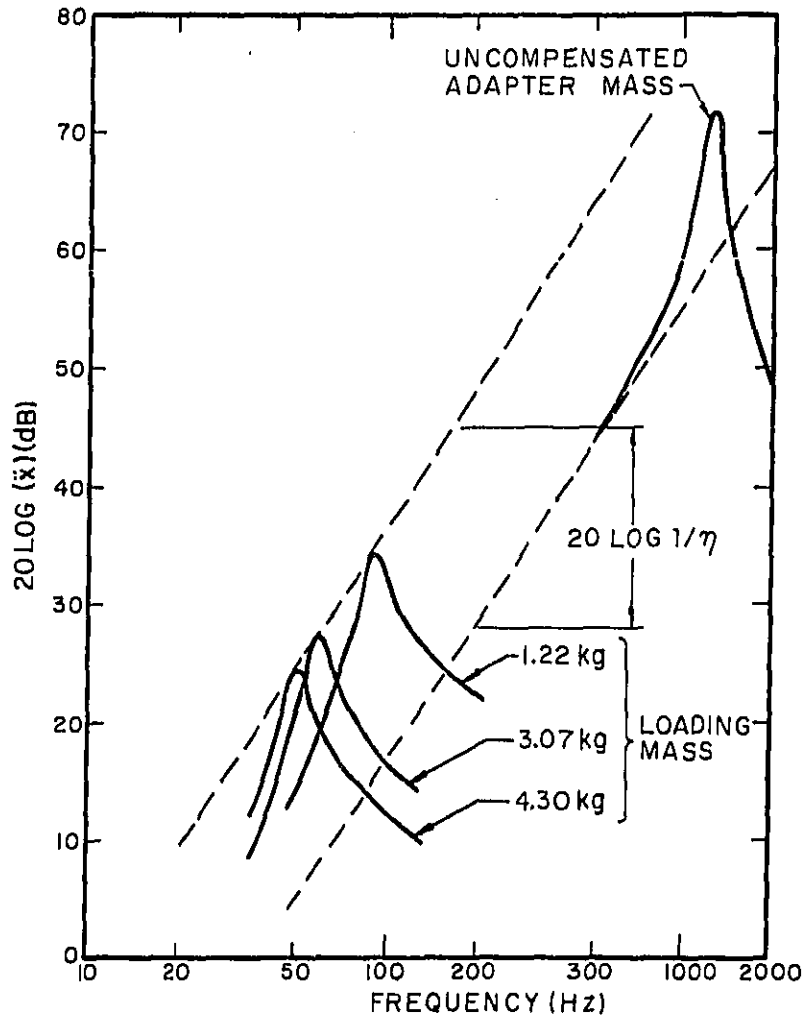

FIG. 13 EVALUATION OF THE LOSS FACTOR FOR A 2"x2"x2" HIGH DENSITY CORK MOUNT

where $\omega_0^2=k/M$, and η is the loss factor of the mount. Dividing Eq. 89 by Eq. 88 provides a convenient method for the evaluation of the loss factor:

$$\frac{|\ddot{x}_{res}|}{|\ddot{x}|} = \frac{1}{\eta} \tag{90}$$

or in logarithmic form:

$$20 \log \eta = 20 \log \frac{|\ddot{x}|}{|\ddot{x}_{res}|} , \tag{91}$$

where $\ddot{x}$, $\ddot{x}_{res}$ and η are evaluated at the resonance frequency f_0.

Figure 13 shows the acceleration response evaluated for three different additional masses: M=4.3, 3.07, and 1.22 kg. The fourth response curve, with the highest peak, is obtained for no additional mass and partial compensation of the adapter mass. According to Eq. 91, the loss factor η can be directly read as the distance in dB between the two dotted lines at frequency f_0 in Fig. 13. The loss factors of the measured mounts are shown in Table I.

TABLE I. Estimated loss factor of the measured vibration isolation mounts.

Description	Size	Average Loss Factor
High density cork	2 in. × 2 in. × 1 in.	0.26
	2 in. × 2 in. × 2 in.	0.206
	2 in. × 2 in. × 3 in.	0.25

TABLE I *(continued)*

Description	Size	Average Loss Factor
Standard density cork	2 in. × 2 in. × 2 in.	0.21
	2 in. × 2 in. × 3 in.	0.23
Low density cork	2 in. × 2 in. × 2 in.	0.19
Precompressed glass-fiber	2 in. × 2 in. × 2 in.	0.15
Neoprene	2 in. × 2 in. × 3 in.	0.195

A detailed description of the measured vibration isolation mounts is given in Appendix I.

F. Anisotropic Behavior of Dynamic Stiffness

In measuring the dynamic stiffness, we observed a pronounced anisotropy of the cork mounts. The dynamic stiffness was 40% to 80% lower when the load was applied at the smooth-surface[a] than at the rough surface (perpendicular to the smooth-surface). The static load deflection curves discussed in Sec. VI confirm these findings. (The dynamic stiffness vs static load curves summarized in Figs. 11 and 12 are those obtained with load applied to the smooth surface of the cork samples.) Therefore, in order to achieve the best performance of the cork mounts, the contractor responsible for the installation should be aware of, and made responsible for, the proper orientation (smooth surfaces horizontal) of the mounts.

[a]The smooth surfaces result from the application of the pressure to these sides during steam curing.

VI. STATIC LOAD-DEFLECTION CURVES

The static load-deflection curves of representative samples were measured by the Korfund Dynamics Corporation. The samples were identical with those used for the evaluation of the dynamic stiffness, as described in Sec. V.

Figure 14 shows the static load-deflection curves for a 2-in. cubic standard-density cork mount measured with two different orientations of the sample. These curves are qualitatively representative for all the measured cork mounts; they demonstrate the anisotropy of the cork mount, and confirm the findings already made in the measurement of dynamic stiffness (see Sec. V.E).

The most controversial feature of all the measured static load-deflection curves of cork mounts is that the curves indicate a "softening" of the mount with increasing static load.[a] This is contrary to the dynamic measurements (see Sec. V.C), which show a definite increase of dynamic stiffness with static load.

Figure 15 shows the static load-deflection curves measured for a 2-in. × 2-in. × 3-in. neoprene mount and a 2-in. × 2-in. × 2-in. precompressed glass-fiber mount. While the load-deflection curve of the neoprene mount seems to be linear, the curve of the precompressed glass-fiber mount shows pronounced stiffening with increasing static load.

If one tries to evaluate the "dynamic stiffness" as the tangent of the load-deflection curve at the required static load, the result would be in complete disagreement with the dynamically

[a] The load-deflection curves published in the Korfund Engineering Manual indicate the same behavior.

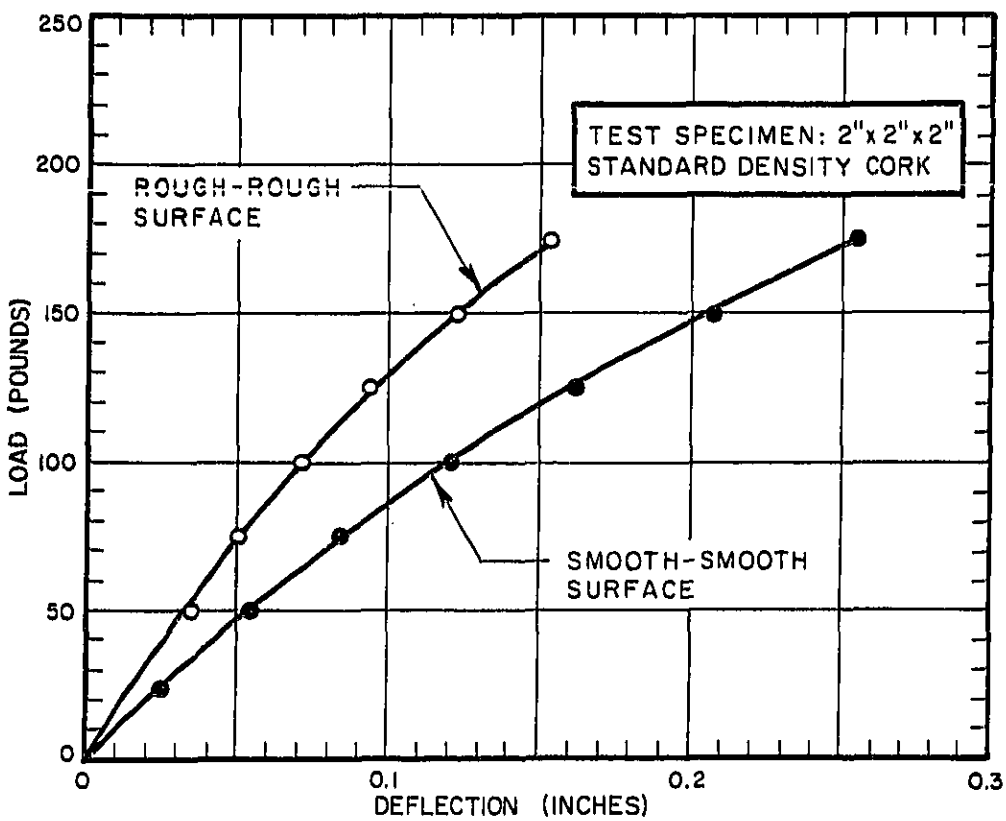

FIG. 14 STATIC LOAD-DEFLECTION CURVE FOR DIFFERENT ORIENTATION OF THE CORK SAMPLE

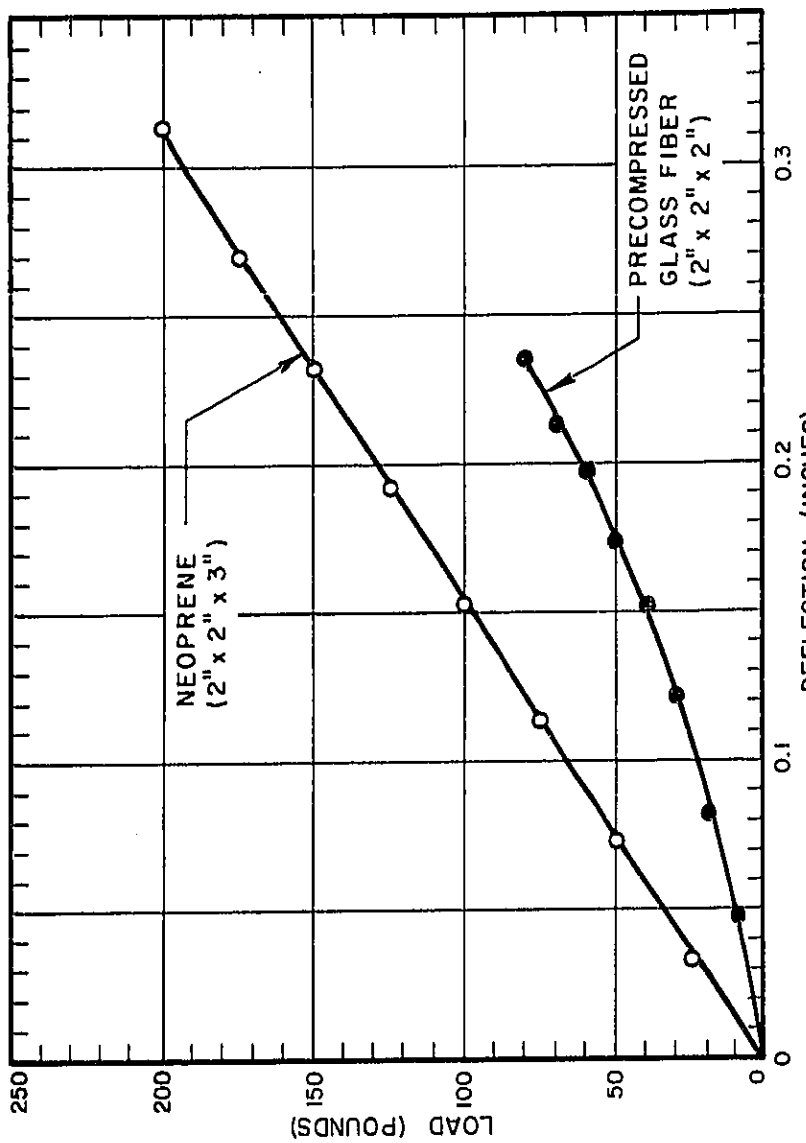

FIG. 15 STATIC LOAD-DEFLECTION CURVES FOR NEOPRENE AND PRECOMPRESSED GLASS FIBER MOUNTS

measured stiffness.[b] This is true not only for the cork but also for the neoprene and precompressed glass-fiber mounts.

Correlation between the static and dynamic stiffnesses could be found only by using the initial slope (taken at small deflections) of the static load-deflection curve. Here the stiffness evaluated from the initial slope was two to three times smaller than the measured dynamic stiffness.

In summary, we conclude that the static load-deflection curve does not provide useful information about the dynamical behavior of the measured mounts. This curve always predicts dynamic stiffnesses too small – with the possibility of errors as large as 500% (e.g., cork under high loading). Consequently, any criteria for the measured mounts based on static deflection under load are irrelevant and should not be used in specifications.

Since the above findings are very much in contrast to common belief and also seem to indicate that the currently recommended design procedures (which are based on the belief that the static load-deflection curve enables one to predict the dynamic behavior) are wrong, the subject needs to be more extensively investigated than it was possible to do in the framework of the present study of floating floors.

[b] Since the dynamic stiffness was measured by two independent methods (impedance head and resonant method), both providing the same result, the correctness of these data is assured.

VII. POINT INPUT ADMITTANCE OF CONCRETE SLABS

In order to evaluate Eqs. 21, 75, 77, 78 and 79, we need the point input admittance of the concrete slab. The input admittance of an infinite uniform, homogeneous plate is given by [5]:

$$Y = \frac{1}{2.3\rho c_L h^2} , \qquad (92)$$

where ρ is the density of the slab material, c_L is the propagation velocity of longitudinal waves in the slab material, and h is the slab thickness. If we insert into Eq. 92 the appropriate values,[a]

Dense Concrete	Lightweight Concrete
$\rho = 2.3\ 10^3$ kg/m^3	$\rho = 6.10^2$ kg/m^3
$c_L = 3.4\ 10^3$ m/sec	$c_L = 1.7\ 10^3$ m/sec ,

we obtain the input admittance,

$$Y_{DENSE} = \frac{8.9\ 10^{-5}}{h^2} \quad (h \text{ in inches, } Y \text{ in } \frac{\text{m/sec}}{\text{Newton}}) \qquad (93)$$

$$Y_{LIGHT} = \frac{6.8\ 10^{-4}}{h^2} \quad (h \text{ in inches, } Y \text{ in } \frac{\text{m/sec}}{\text{Newton}}) . \qquad (94)$$

Equations 93 and 94 are plotted in Fig. 16.

[a] 1m = 40 in., 1 Newton $\doteq$ 0.225 lb_{force}.

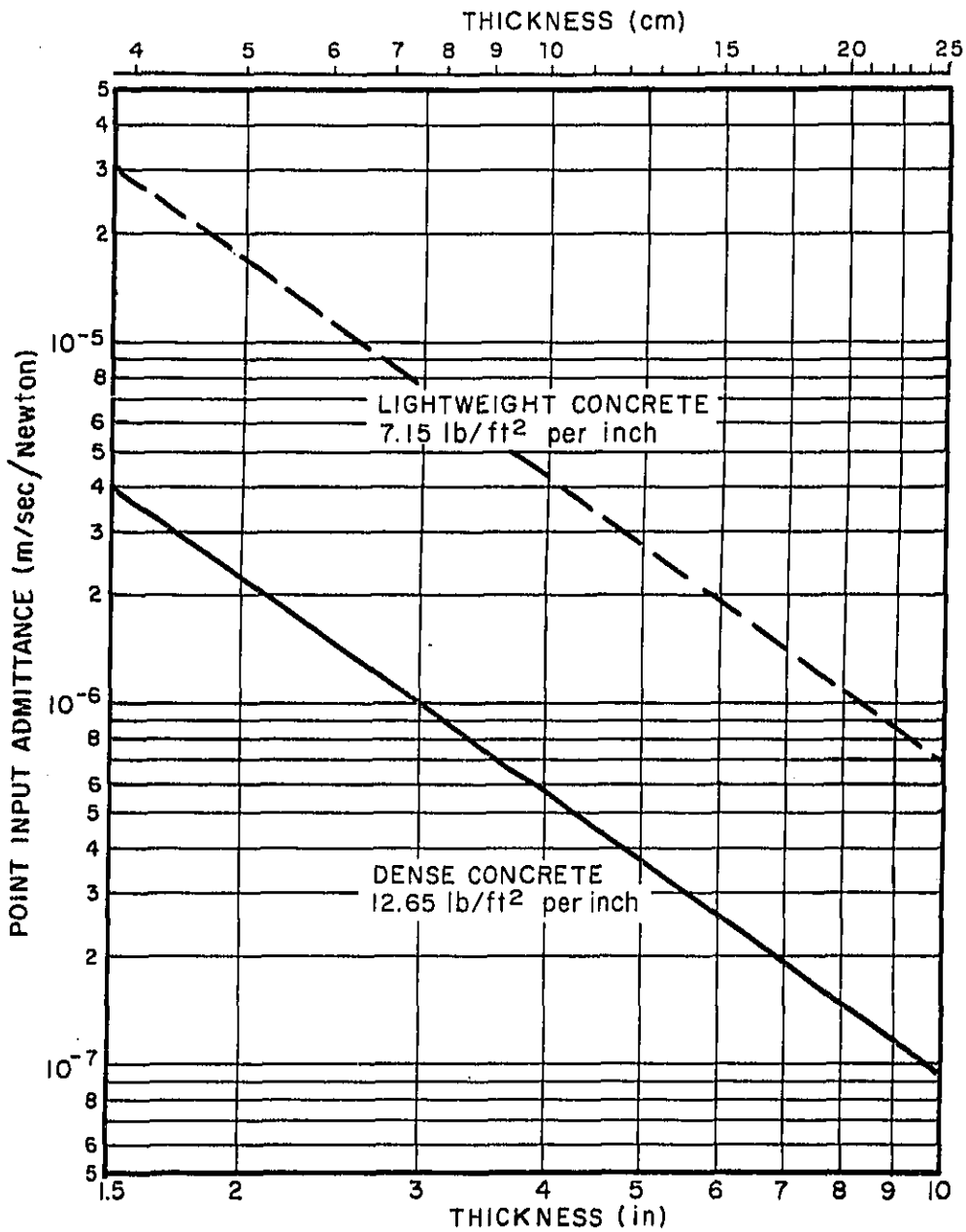

FIG. 16 POINT INPUT ADMITTANCE OF "INFINITE" CONCRETE SLABS AS A FUNCTION OF SLAB THICKNESS

VIII. CALCULATION OF A CONCRETE EXAMPLE

In order to demonstrate how to use the results of the previous Sections, we shall calculate the acoustical performance of a floating floor system consisting of an 8-in.-thick structural slab and a 4-in.-thick floating slab, both of dense concrete. The floating slab is supported on standard-density cork mounts, of 2 in. × 2 in. × 2 in. dimensions. The airspace between the slabs is assumed to be filled with low-density (e.g., 0.5 lb/ft^3) glass fiber, as shown schematically in the following sketch.

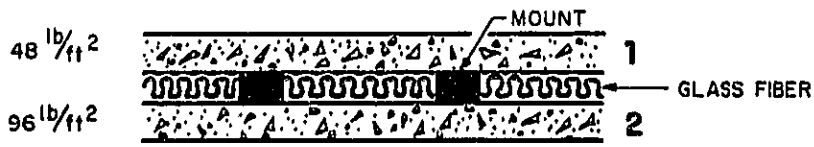

SK-3. Sketch of the floating floor.

A. Calculation of the Basic Resonance Frequency

The surface weight of the slabs is:

$$W_{s_4} = 144 \text{ lb/ft}^3 \times \frac{4}{12} \text{ ft} = 48 \text{ lb/ft}^2$$

and

$$W_{s_8} = 96 \text{ lb/ft}^2 \ .$$

Accordingly,

$$W_s = \frac{W_{s_4} \times W_{s_8}}{W_{s_4} + W_{s_8}} = \frac{4.6 \times 10^3}{1.44 \times 10^2} = 32 \text{ lb/ft}^2 .$$

The lowest possible resonance frequency can either be calculated from Eq. 12b, or can be obtained directly from Fig. 1:

$$f_{00} = \frac{140}{\sqrt{d_0 W_s}} = \frac{140}{\sqrt{2 \times 32}} = 17.7 \text{ Hz} .$$

The weight of $1m^2$ of floating slab is[a]

$$W = 48 \times 10.76 = 516 \text{ lb/m}^2 .$$

Since the rated load of the standard density 2 in. × 2 in. × 2 in. cork mount is 133 lb, the number of mounts per m^2 of slab area is

$$n' = \frac{516 \text{ lb/m}^2}{133 \text{ lb}} = 3.89 \frac{1}{m^2} \approx 4 \frac{1}{m^2} .$$

The dynamic stiffness of the standard density cork mount under the rated load (133 lb) can be approximated from Fig. 11:

$$k = 4.5 \times 10^3 \text{ lb/in.} = 8 \times 10^5 \text{ N/m}^b .$$

The stiffness of the mounts, per $1m^2$ of a slab area, is four times the stiffness of a single mount:

$$n'k = 4 \times 4.5 \times 10^3 = 1.8 \times 10^4 \text{ lb/in.} = 3.2\ 10^6 \text{ N/m} .$$

The dynamic stiffness of the trapped air per square meter of slab

---

[a] $1m^2 = 10.76 \text{ ft}^2$.

[b] $1 \text{ lb/in.} = 1.78\ 10^2 \text{ N/m}$.

area is obtained from Fig. 2:

$$k_0 = 1.07 \times 10^4 \text{ lb/in.} = 1.9\ 10^6 \text{ N/m} .$$

The actual natural frequency of the floated floor system is calculated according to Eq. 14b:

$$f_0 = f_{00} \sqrt{1 + \frac{n'k}{k_0}} = 17.5 \sqrt{1 + \frac{1.8}{1.07}} = 28.8 \text{ Hz} .$$

B. Calculation of the Improvement in Sound Transmission Loss (ΔTL)

The improvement in sound transmission loss over the single slab, ΔTL, is given in Eq. 76b. In order to evaluate this equation, we first have to calculate $K_{12}(\omega)$, as given in Eq. 22:

$$K_{12}(\omega) = \frac{|Z|^2 Y_2}{1+2\mathrm{Re}\{Z\}(Y_1+Y_2)+|Z|^2 (Y_1+Y_2)^2} .$$

Since the real part of the impedance of the mount is small compared with the imaginary part, we can reasonably assume that

$$Z \approx i \frac{k}{\omega} + r \approx i \frac{k}{\omega} = i \frac{8 \times 10^5}{2\pi f} \cdot \frac{\text{N/m}}{\text{1/sec}} ,$$

$$|Z| = \frac{1.27 \times 10^5}{f} \frac{\text{Nsec}}{\text{m}} ,$$

$$|Z|^2 = \frac{1.62 \times 10^{10}}{f^2} \left(\frac{\text{Nsec}}{\text{m}}\right),$$

from Sec. V:

$$r = \eta \frac{k}{\omega}$$

$$\eta = 0.21$$

and

$$\mathrm{Re}\{Z\} \approx \eta|Z| = 0.21 \times \frac{1.27 \times 10^5}{f} = \frac{2.67 \times 10^4}{f} \frac{\text{Nsec}}{\text{m}} .$$

The point input admittances, Y_1 and Y_2, can be calculated from Eq. 93 or obtained directly from Fig. 16:

$$Y_1 = 5.55 \times 10^{-6} \frac{\text{m}}{\text{secN}} ,$$

$$Y_2 = 1.39 \times 10^{-6} \frac{\text{m}}{\text{secN}} ,$$

$$Y_1+Y_2 = 6.94 \times 10^{-6} \frac{\text{m}}{\text{secN}} ,$$

$$(Y_1+Y_2)^2 = 4.8 \times 10^{-11} \left(\frac{\text{m}}{\text{secN}}\right)^2 .$$

Accordingly,

$$K_{12}(\omega) = \frac{\frac{1.62}{f^2} \times 10^{10} \; 1.39 \times 10^{-6}}{1 + 2 \frac{2.67 \times 10^4}{f} 6.94 \times 10^{-6} + \frac{1.62 \times 10^{10}}{f^2} \times 4.8 \times 10^{-11}}$$

$$K_{12}(\omega) = \frac{2.26 \times 10^4 \; \frac{1}{f^2}}{1 + 0.38 \frac{1}{f} + 0.78 \frac{1}{f^2}} \approx \frac{2.26 \times 10^4}{f^2} ,$$

which shows that, for floated floor applications, $K_{12}(\omega)$ can be simplified to

$$K_{12}(\omega) \approx |Z|^2 Y_2 .$$

Inspecting the former numerical result, we see that

$$K_{12}(\omega) > 1 \qquad \text{if} \quad f < 150 \text{ Hz} ,$$

and

$$K_{12}(\omega) < 1 \qquad \text{if} \quad f > 150 \text{ Hz} .$$

Using the material constants listed below, we can numerically evaluate the various terms in Eq. 77:

$c_0 = 340$ m/sec $\qquad\qquad \eta_1 = \eta_2 = 10^{-2}$

$c_L = 3.4 \times 10^3$ m/sec $\qquad\qquad n' = 4 \frac{1}{m^2}$

$\rho = 2.3 \times 10^3$ kg/m^3 $\qquad\qquad k = 8.10^5 \frac{N}{m}$

$\rho_{s_1} = 2.3 \times 10^2$ kg/m^2 $\qquad\qquad K_{12}(\omega) = \frac{2.26 \times 10^4}{f^2} \frac{\text{Nsec}}{m}$

$\rho_{s_2} = 4.6 \times 10^2$ kg/m^2

Now we start the numerical evaluation of Eq. 77 by calculating the respective terms of the numerator and the denominator separately.

The first term in the numerator is:

$$\left(\frac{\sqrt{\pi}}{\rho_s \omega}\right)^2 = \left(\frac{\sqrt{\pi}}{4.6\ 10^2 \times 2\pi f}\right)^2 = \left(\frac{1}{1.65\ 10^3 f}\right)^2 = \frac{3.6 \times 10^{-7}}{f^2} .$$

Assuming a loss factor of $\eta_2 = 0.01$, we find that the second term in the numerator becomes

$$\frac{\pi\sqrt{12}\, c_0^2\sigma_{rad_2}^2}{2c_{L_2}h_2\rho_{S_2}^2\eta_2\omega^3} = \frac{\pi\sqrt{12}\,(3.4\times10^2)^2\,\sigma_{rad_2}^2}{2\times(3.4\ 10^3)\times0.2\times(4.6\times10^2)^2\times0.01\times8\pi^3f^3}$$

$$= \frac{1.75\ 10^{-3}}{f^3}\,\sigma_{rad_2}^2 \ .$$

Comparing the above two terms, we notice that below 4.9 kHz the resonant contribution is large compared with the forced contribution.

The first term of the denominator is

$$\left[\frac{n'k}{\rho_{S_1}\rho_{S_2}\omega^3}\right]^2 = \left[\frac{4\times(8\times10^5)}{(2.3\times10^2)(4.6\times10^2)8\pi^3f^3}\right]^2 = \frac{1.48\ 10^{-2}}{f^6} \ .$$

The second term of the denominator is

$$\frac{\pi\sqrt{12}\, c_0^2\ \sigma_{rad_1}\sigma_{rad_2}}{2c_{L_1}h_1\rho_{S_1}\rho_{S_2}\eta_2\omega^3} \times \frac{1}{1+\frac{\rho_{S_1}}{\rho_{S_2}}\frac{Y_1}{Y_2}\frac{\eta_1}{\eta_2}+\frac{\rho_{S_1}\omega\eta_1}{K_{12}(\omega)n'}} \ .$$

The first part of the second term of the denominator is $(\rho_{S_2}h_2)/(\rho_{S_1}h_1)$ times the second term of the numerator (already calculated).

$$\frac{\pi\sqrt{12}\, c_0^2\ \sigma_{rad_1}\sigma_{rad_2}}{2c_{L_1}h_1\rho_{S_1}\rho_{S_2}\eta_2\omega^3} = \frac{7\ 10^{-3}}{f^3}\,\sigma_{rad_1}\sigma_{rad_2} \ .$$

If we assume $\eta_1=10^{-2}$, the second part of the second denominator term gives

$$\frac{1}{\left(1 + \frac{\rho_{s_1}}{\rho_{s_2}} \frac{Y_1}{Y_2} \frac{\eta_1}{\eta_2} + \frac{\rho_{s_1} \omega \eta_1}{K_{12}(\omega) n'}\right)} = \frac{1}{\left(1 + \frac{1}{2} \frac{4}{1} \frac{1}{1} + \frac{(2.3\ 10^2) \times 2\pi f \times 10^{-2}}{\frac{2.26 \times 10^4}{f^2} \times 4}\right)}$$

$$= \frac{1}{3 + 1.6\ 10^{-4}\ f^3} ,$$

which, for $f > 26$ Hz, reduces to $(6.25 \times 10^3)/(f^3)$.

Putting the previously evaluated terms into Eq. 77, we obtain, for the improvement in sound transmission loss over the single slab,

$$\Delta TL \approx 10 \log \left[\frac{\frac{3.6\ 10^{-7}}{f^2} + \frac{1.75\ 10^{-3}}{f^3} \sigma^2_{rad_2}}{\frac{1.48\ 10^{-2}}{f^6} + 4 \times \frac{1.75\ 10^{-3}}{f^3} \times \frac{6.25\ 10^3}{f^3} \sigma_{rad_1} \sigma_{rad_2}} \right] .$$

Since the first terms in the numerator as well as in the denominator are small compared with their respective second terms, the ΔTL can be approximated by

$$\Delta TL \approx 10 \log \left[\frac{\sigma_{rad_2}}{\sigma_{rad_1}} \frac{f^3}{4 \times 6.25\ 10^3} \right] = 10 \log \left[4 \times 10^{-5} \frac{\sigma_{rad_2}}{\sigma_{rad_1}} f^3 \right] ,$$

$$\Delta TL \approx -44 \text{ dB} + 10 \log \frac{\sigma_{rad_2}}{\sigma_{rad_1}} + 30 \log f .$$

Figure 17 shows the calculated improvement in sound transmission loss for $\sigma_{rad_2} = \sigma_{rad_1} = 1$.

The rapid increase of ΔTL with increasing frequency implies a very large improvement at high frequencies. This improvement, however, usually cannot be fully realized because of flanking transmission. The next Section of this report gives a brief treatment of the flanking problem.

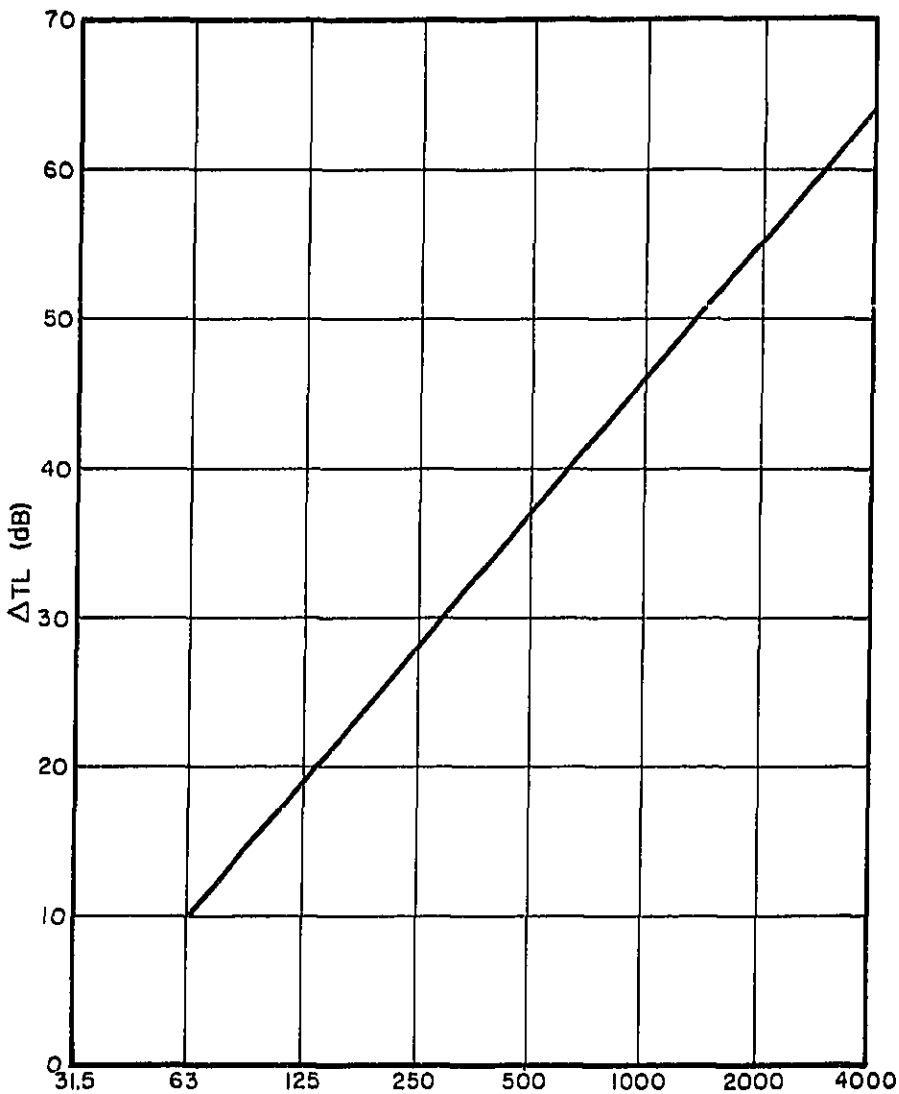

FIG. 17 CALCULATED ΔTL VS. FREQUENCY

IX. DISCUSSION ON FLANKING TRANSMISSION

It is common knowledge that the improvement of sound transmission loss for floating floors is limited by flanking transmission through structural elements common to the source and receiving rooms. Figure 18 shows the three principal paths of sound transmission between the source and receiving rooms. Path 1 represents the direct sound transmission through the floating floor system. The sound transmission loss through this path was calculated in Sec. IV. Path 2 represents the flanking transmission through the walls common to the source and receiving rooms. This is the flanking path mainly responsible for limitation of the potential performance of a floating floor system. Path 3 represents the flanking through the walls of the source room into the structural slab, which in turn radiates sound into the receiving room.

One of the first treatments of flanking transmission was given by Meyer *et al.* [6], in a paper presenting measured data and a qualitative theory. Westphal [7], in a subsequent work, presented measured data obtained in a variety of buildings. Kihlman [8] has derived a theoretical solution for the transmission of incident bending waves at the junction of semi-infinite plates. Gösele [9], in a recent work, has reviewed the flanking transmission problem and has given an engineering formula for the calculation of bending wave transmission through a junction. According to Gösele's formula, which agrees with measured results, the velocity transmission factor, γ, through Path 2 (see Fig. 18) is

$$\gamma = 10 \log \frac{\langle v_S^2 \rangle}{\langle v_R^2 \rangle} = 20 \log \frac{W_{kd}}{W_{ng}} + 12 \text{ dB} , \qquad (95)$$

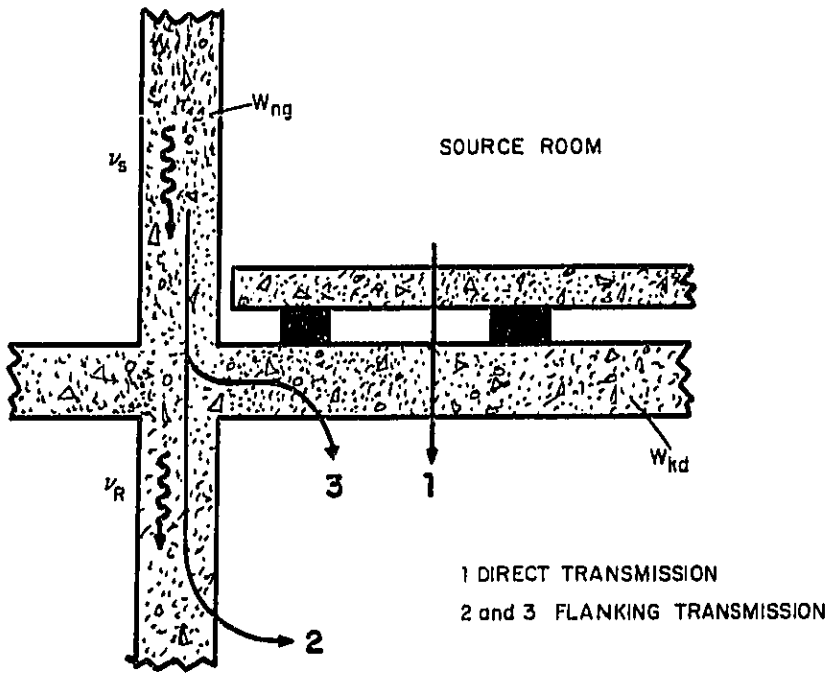

FIG. 18 PRINCIPAL PATHS OF SOUND ENERGY TRANSMISSION BETWEEN SOURCE AND RECEIVING ROOM

where $\langle v_S^2 \rangle$ = the space-average squared velocity of the flanking wall in the source room

$\langle v_R^2 \rangle$ = the space-average squared velocity of the flanking partition in the receiving room

W_{kd} = the surface weight of the flanked partition (in our case, the structural slab only[a])

W_{ng} = the surface weight of the flanking partition (the wall in our case).

Using Gösele's engineering approximation for the velocity transmission factor, one can calculate a so-called flanking transmission loss TL_f[b]:

$$TL_f = 10 \log \frac{\pi_0}{\pi_f} = TL_{ng} + 10 \log \frac{A_{kd}}{A_{ng}} + 20 \log \frac{W_{kd}}{W_{ng}} + 12 \ , \qquad (96)$$

where π_0 = the sound power incident on the flanked partition due to the airborne sound field in the source room

π_f = the sound power radiated into the receiving room through flanking Path 2

TL_{ng} = the sound transmission loss of the flanking partition

A_{kd} = the surface area of the flanked partition (the structural floor slab)

A_{ng} = the surface area of all flanking partitions in the receiving room (four walls, in our case).

[a] Above the basic resonance frequency of the floating slab system, the floating slab is dynamically decoupled from the structural slab.

[b] The derivation of Eq. 96 is given in Appendix II.

For convenience in evaluation of Eq. 96:

$$\Psi = 20 \log \frac{W_{kd}}{W_{ng}} + 12 \text{ is plotted in Fig. 19.}$$

The "Flanking-Sound Transmission Loss", as defined in Eq. 96, is directly comparable with the TL of the flanked partition (e.g., if TL_f is less than TL, the partition is flanked).

As an example, let us calculate the "Flanking-Sound Transmission Loss" at a frequency of 1000 Hz for a construction consisting of a 4-in. floating slab resiliently supported on a 12-in. dense concrete structural slab, with flanking walls made of 12-in. dense concrete. From Fig. 6, we get the TL of the 12-in. wall at 1000 Hz:

$$TL_{ng} = 62 \text{ dB} .$$

Since $W_{kd}/W_{ng} = 1$, Fig. 19 gives $\Psi = 12$. Further, assuming that the surface area of the four flanking walls, A_{ng}, is 2.5 times the area of the structural slab, we obtain, from Eq. 96,

$$TL_f = 62 + 10 \log \frac{1}{2.5} + 12 = 70 \text{ d B.}$$

This means that the flanking transmission will not permit us to realize more than 8 dB improvement in sound transmission loss by adding the 4-in. floating slab to the 12-in. structural slab. This example clearly indicates that an expensive floating floor construction, intended to increase the sound transmission loss of a structural floor, is not justifiable if the flanking transmission is not reduced at the same time. It should be noted that *vibration isolation* of a floating floor *is not subject to flanking,* since the floating slab does not have any rigid connection

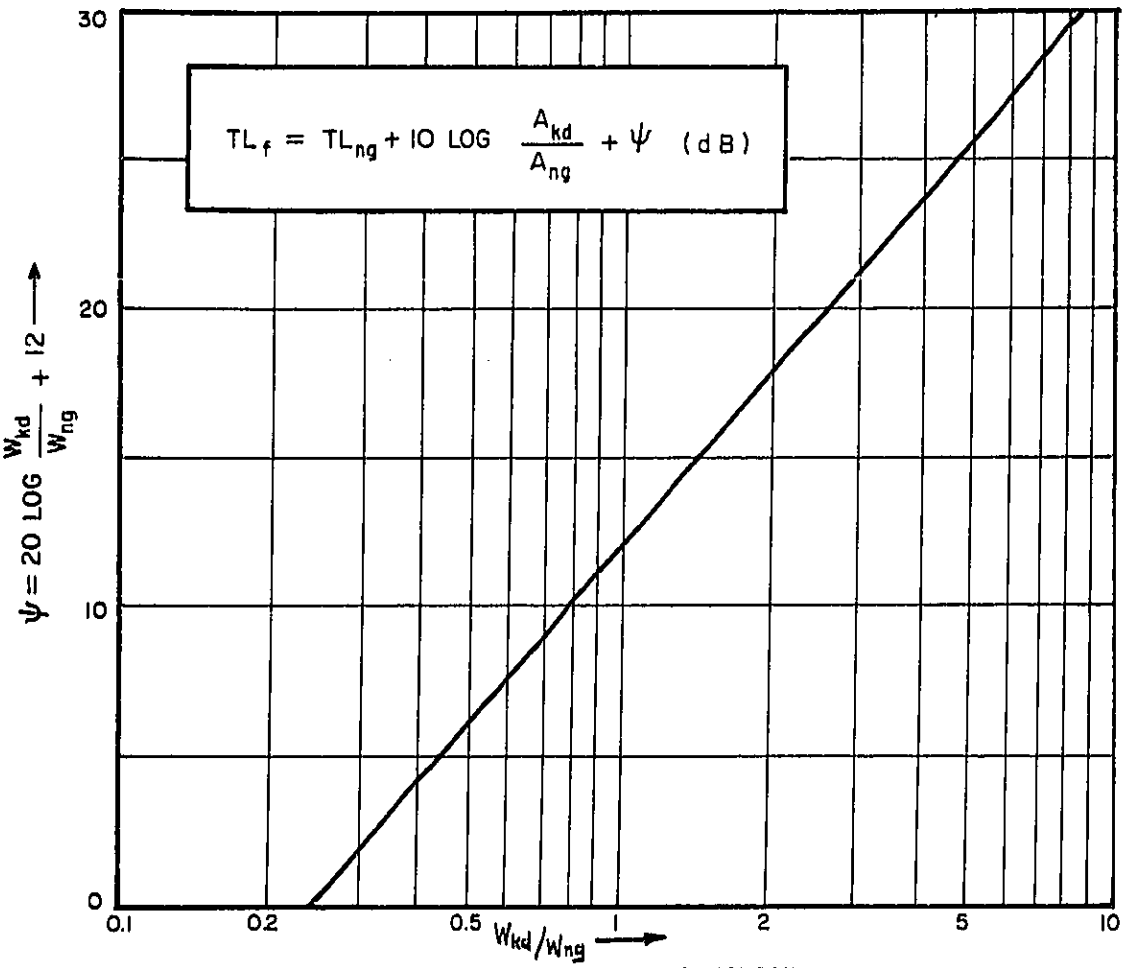

TL_{ng} = TL OF FLANKING PARTITION
A_{kd} = SURFACE AREA OF FLANKED PARTITION
A_{ng} = SURFACE AREA OF FLANKING PARTITIONS IN SOURCE ROOM
W_{kd} = SURFACE WEIGHT OF FLANKED PARTITION
W_{ng} = SURFACE WEIGHT OF FLANKING PARTITION

FIG. 19 GRAPH FOR THE ESTIMATION OF THE FLANKING TRANSMISSION LOSS TL_f

to the walls. The concluding Section contains advice for the reduction of flanking transmission.

X. VIBRATIONAL AND ACOUSTICAL RESPONSE TO POINT-FORCE EXCITATION

In the preceding Sections we have calculated the response of a single slab and a floating floor system to acoustical excitation. In many applications, however, the floor is excited by vibrational forces as well as by airborne sound field. It is of interest to know the vibration response of the floor system to such forces, for, with this knowledge one can calculate the sound power radiated by the floor into the room below. The point force gives a good approximation for the vibration forces transmitted to the floor by the supports of the machines.

A. Single Slab

When a point force F is applied to a slab, the power, π_s, transmitted into the slab is given by

$$\pi_s(x) = F^2 Y(x) \ , \qquad (97)$$

where Y(x) is the point input admittance of the slab at the excitation point x. In order to simplify the analysis, we again assume that the point input admittance of the finite floor can be approximated by the point input admittance Y_∞ of an infinite slab of the same thickness; Y_∞ is real and independent of frequency. This assumption is valid only at high frequencies. At low frequencies one has to calculate or measure the point input admittance at the point of excitation. While Y(x) for the finite slab fluctuates strongly with position, the space average of Y(x) equals the point input admittance of the infinite floor Y_∞. Accordingly, even at low frequencies, Y_∞ is a good approximation for Y(x). Using the input admittance of the infinite floor in Eq. 97,

we obtain the following approximation:

$$\pi_s = F^2 Y_\infty \quad . \tag{98}$$

This power supplied to the slab must be equal to the power lost in the slab, π_η, plus the power radiated as airborne sound by the slab, π_{rad}. The power balance of the slab can be written as

$$\pi_s = F^2 Y_\infty = \pi_\eta + \pi_{rad} \quad . \tag{99}$$

Using the nomenclature introduced in Sec. IV.B.1, we obtain

$$F^2 Y_\infty = \langle v^2 \rangle \rho_s A \omega \eta + \langle v^2 \rangle \rho_0 c_0 A \sigma_{rad} \quad , \tag{100}$$

which immediately yields the space-time average squared velocity,

$$\langle v^2 \rangle = \frac{F^2 Y_\infty}{A(\rho_s \omega \eta + \rho_0 c_0 \sigma_{rad})} \quad . \tag{101}$$

It should be noted here that the loss factor η represents both the internal viscous losses in the slab material, and the power lost through conduction of vibration energy into adjoining structural elements. At low frequencies usually the latter loss mechanism is the dominant one.

The sound power radiated by the slab into the room below is given by

$$\pi_1 = \langle v^2 \rangle \rho_0 c_0 A \sigma_{rad} = F^2 Y_\infty \frac{\rho_0 c_0 \sigma_{rad}}{\rho_s \omega \eta + \rho_0 c_0 \sigma_{rad}} \quad . \tag{102}$$

Since the power lost by radiation is usually negligible compared with the other losses, we obtain[a]

$$\pi_1 \approx F^2 Y_\infty \frac{\rho_0 c_0 \sigma_{rad}}{\rho_s \omega \eta} . \qquad (103)$$

Further, we have already given the point input admittance of an infinite, uniform, homogeneous slab of thickness h in Eq. 92 as:

$$Y_\infty = \frac{1}{2.3\ \rho c_L h^2} . \qquad (104)$$

Using Eq. 104 and considering $\rho_s = \rho h$, Eq. 103 reduces to:

$$\pi_1 = F^2 \frac{\rho_0 c_0 \sigma_{rad}}{2.3\ \rho^2 c_L \eta h^3 \omega} . \qquad (105)$$

Using $\pi_0 = 10^{-12}$ watts as reference, we get the follow equation for the power level of the sound radiated into the receiving room:

$$PWL = 10 \log \frac{\pi_1}{\pi_0} = 10 \log \left[\frac{F^2 \frac{\rho_0 c_0 \sigma_{rad}}{2.3\ \rho^2 c_L \eta h^3 \omega}}{10^{-12}} \right] . \qquad (106)$$

Inserting the appropriate values for the constants for dense

---

[a] Note that the surface area of the slab is canceled out. The influence of the surface area is, however, still contained in the loss factor which decreases with increasing slab area (i.e., as the area-to-perimeter ratio increases). Below the coincidence frequency of the slab, σ_{rad} also depends on the surface area.

conrete, $\rho = 2.3\ 10^3$ kg/m^3

$c_L = 3.4\ 10^3$ m/sec

$\rho_0 c_0 = 400$ mks rayls ,

we find that Eq. 106 yields, in mks units (F_N in Newtons, h_m in meters),[a]

$$PWL_{re\ 10^{-12}\,W} = 20 \log F_N + 10 \log \sigma_{rad} - 10 \log \eta + \theta_N \ , \qquad (107)$$

with

$$\theta_N = 32 - 30 \log h_m - 10 \log f \ . \qquad (108)$$

In English units (F_{lb} in pounds; h_{in} in inches) we get

$$PWL(\text{re } 10^{-12} \text{ Watts}) = 20 \log F_{lb} + 10 \log \sigma_{rad} - 10 \log \eta + \theta_{lb} \ , \qquad (109)$$

when

$$\theta_{lb} = 93 - 30 \log h_{in} - 10 \log f \ . \qquad (110)$$

To speed up calculation, we have plotted θ_N and θ_{lb} in Fig. 20.

In calculating a concrete example, one reads the respective value for θ from Fig. 18 and adds 10 log F + 10 log σ_{rad} - 10 log η (with F in the appropriate units). The radiation efficiency term 10 log σ_{rad} is zero above the coincidence frequency[b] of the slab; below the coincidence frequency it can be evaluated from Fig. 5.

---

[a] 1 Newton = 0.225 lb_f ; 1m = 40 in.

[b] The coincidence frequency is given as a function of slab thickness in Fig. 4.

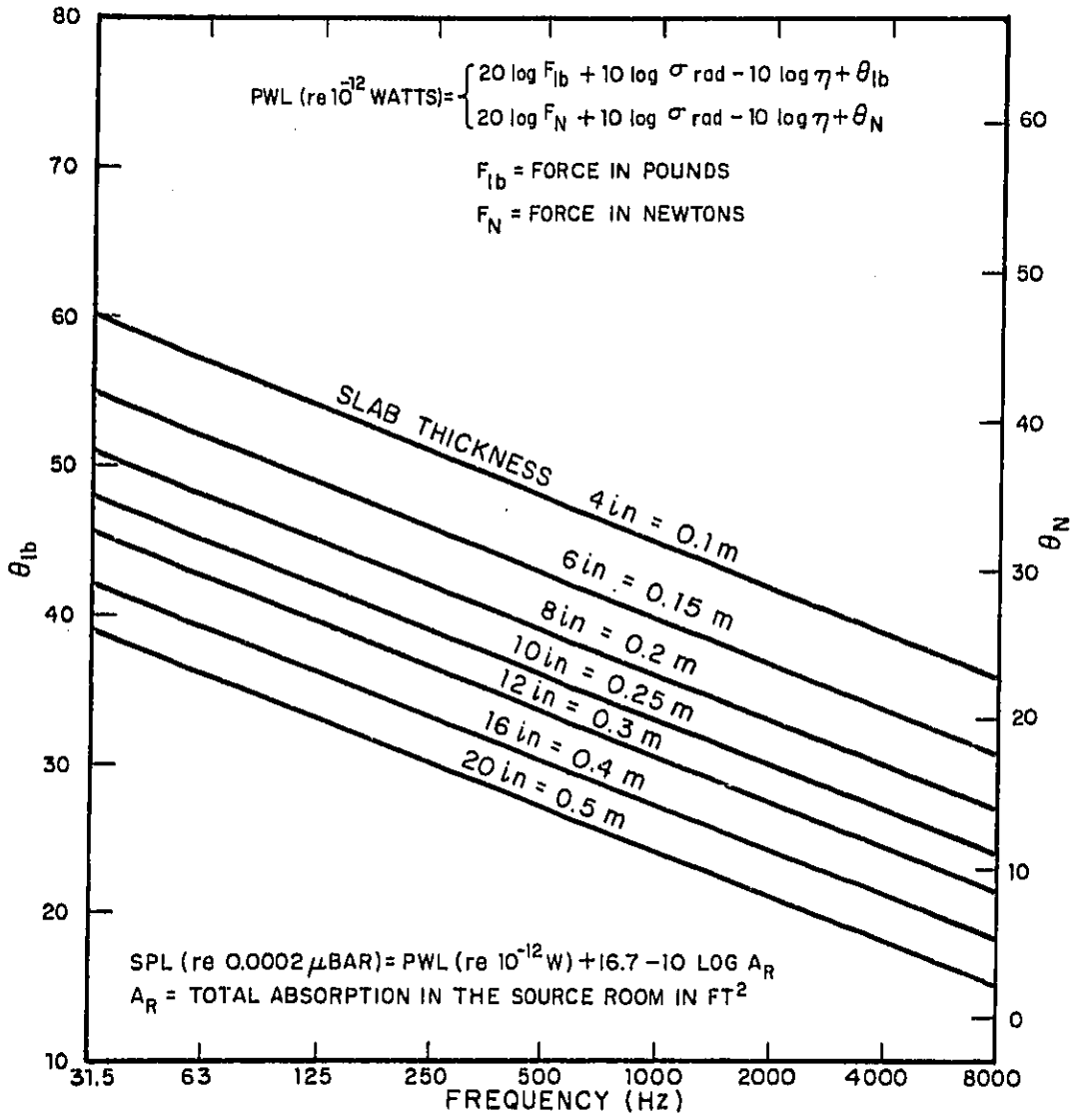

FIG. 20 GRAPH TO CLACULATE THE SOUND POWER LEVEL OF DENSE CONCRETE SLABS FOR POINT FORCE EXCITATION

As an example, let us evaluate the sound power level of an 8-in.-thick dense concrete slab for a vibration point force of 10 lb at a frequency of 1000 Hz and η=0.01. From Fig. 18 we get Θ_{lb}=36. Since f>f_c, 10 log σ_{rad} = 0, 20 log F = 20 log 10 = 20, and 10 log η = 10 log 0.01 = - 20.

Thus, the sound power radiated by an 8-in.-thick slab excited by a 10-lb force at 1000 Hz is

$$PWL = 20 + 0 + 20 + 36 = 76 \text{ dB (re } 10^{-12} \text{ Watts)} .$$

B. Floating Slab System

Having calculated the response to point-force excitation of a single slab, we are interested in knowing how much can be gained by adding a floating slab. It is reasonable to assume that the point input impedance of the floating slab well above the basic resonance frequency (given in Eq. 14) is not influenced considerably by the soft vibration isolation mounts. Accordingly, the power injected by the point force into the floating slab is

$$\pi_1 = F^2 Y_1 . \qquad (111)$$

This injected power is partly dissipated in the slab itself through viscous losses,[a] partly transmitted through the isolators to the structural slab, and partly radiated as sound. A part of the power transmitted through a mount into the structural slab will re-enter the floating slab through the other mounts. The

[a] Since the floating slab has no rigid connection to the rest of the structure, its loss factor is always smaller than that of the structural slab.

power balance reads

$$\pi_1 = \pi_{\eta_1} + \pi_{12} + \pi_{1\,rad} - \pi_{21} , \tag{112}$$

where π_1 = power supplied to the floating slab by the point force

π_{η_1} = power lost in the floating slab due to its internal damping

π_{12} = power transmitted from the floating slab to the structural slab through the isolators

π_{1rad} = acoustical power radiated by the floating slab

π_{21} = power transmitted from the structural slab back into the floating slab.

With the nomenclature introduced in Sec. IV, Eqs. 111 and 112 yield

$$F^2 Y_1 = \langle v_1^2 \rangle A \left[K_{12}(\omega) n' + \rho_{s_1} \omega \eta_1 + \rho_0 c_0 \sigma_{rad_1} \right] + \langle v_2^2 \rangle A \frac{Y_1}{Y_2} K_{12}(\omega) n' . \tag{113}$$

The power balance of the structural slab is

$$\pi_{12} = \pi_{\eta_2} + \pi_{rad_2} + \pi_{21} \tag{114}$$

or,

$$\langle v_1^2 \rangle A K_{12}(\omega) n' = \langle v_2^2 \rangle A \left[\rho_{s_2} \omega \eta_2 + \rho_0 c_0 \sigma_{rad_2} + \frac{Y_1}{Y_2} K_{12}(\omega) n' \right] , \tag{115}$$

which yields

$$\langle v_2^2 \rangle = \langle v_1^2 \rangle \frac{K_{12}(\omega)n'}{\rho_{s_2}\omega\eta_2+\rho_0 c_0 \sigma_{rad_2} + \frac{Y_1}{Y_2} K_{12}(\omega)n'} . \qquad (116)$$

Inserting this into Eq. 113, solving for $\langle v_1^2 \rangle$ and putting back $\langle v_1^2 \rangle$ into Eq. 116 gives

$$\langle v_2^2 \rangle = \frac{K_{12}(\omega)n'}{\left[\rho_{s_2}\omega\eta_2+\rho_0 c_0 \sigma_{rad_2} + \frac{Y_1}{Y_2} K_{12}(\omega)n'\right]} \times \frac{\frac{F^2 Y_1}{A}}{\left[\rho_{s_1}\omega\eta_1+\rho_0 c_0 \sigma_{rad}+K_{12}(\omega)n' - \frac{\left(\frac{Y_1}{Y_2}\right)[K_{12}(\omega)n']^2}{\rho_{s_2}\omega\eta_2+\rho_0 c_0 \sigma_{rad_2} + \left(\frac{Y_1}{Y_2}\right)K_{12}(\omega)n'}\right]} \qquad (117)$$

Neglecting the radiation loss terms and multiplying by $\rho_0 c_0 \sigma_{rad_2} A$ gives the sound power radiated into the source room:

$$\pi'_{2a} = F^2 Y_1 \frac{\rho_0 c_0 \sigma_{rad_2}}{\rho_{s_2}\omega\eta_2} \frac{1}{1 + \frac{\rho_{s_1}}{\rho_{s_2}} \frac{Y_1}{Y_2} \frac{\eta_1}{\eta_2} + \frac{\rho_{s_1}\omega\eta_1}{K_{12}(\omega)n'}} . \qquad (118)$$

The improvement in performance over the single slab is the logarithmic ratio of the acoustic power radiated in the source room by the single and composite slabs (as given in Eqs. 103 and 118, respectively).

$$\text{Improvement} = 10 \log \frac{\pi_{2a}}{\pi'_{2a}} = 10 \log \left[\frac{Y_2}{Y_1} \left(1 + \frac{\rho_{s_1}}{\rho_{s_2}} \frac{Y_1}{Y_2} \frac{\eta_1}{\eta_2} + \frac{\rho_{s_1} \omega \eta_1}{K_{12}(\omega) n^r} \right) \right] . \tag{119}$$

If both slabs are of the same material, Eq. 119 simplifies to

$$\text{Improvement} = 10 \log \left[\frac{h_1^2}{h_2^2} \left(1 + \frac{h_1}{h_2} \frac{\eta_1}{\eta_2} + \frac{\rho_{s_1} \omega \eta_1}{K_{12}(\omega) n^r} \right) \right] . \tag{120}$$

Comparing Eq. 120 with Eq. 77, we notice that the improvement to be exactly the same as ΔTL, if one neglects the contribution of the forced terms in Eq. 77. The practical example calculated in Sec. VIII showed that in fact these terms are negligible compared with the resonant terms. Accordingly, the improvement for point-force excitation and ΔTL are practically identical.

Equation 120 again demonstrates the importance of high loss factor for the performance of a floating floor. It is recommended that further research should be directed to find practical methods for the construction of floating slabs of high viscous losses. In contrast to the sound isolation performance of the floating floor system, the vibration isolation performance is not subject to flanking, since the floating slab does not have rigid connection to walls.

XI. CONCLUSIONS AND RECOMMENDATIONS

As a result of the study described in this report, theoretical methods for the calculation of sound and vibration isolation properties of single and floating floors have been developed. The most important results are presented in graphical form, to give the designer a quick grasp of the somewhat complicated equations.

The theoretical calculations show that the stiffness of the trapped air sets a lower limit for the basic resonance frequency of the floating floor. The low resonance frequencies often claimed for very soft mounts, such as precompressed glass-fiber, usually neglect the stiffness of the air. Such a low resonance frequency may be realizable in isolating individual items of small equipment, but in floated floor applications, where the air is trapped between the slabs, it is completely unrealistic.

Our measurements of the dynamic stiffness of various elastic floor mounts, such as cork, neoprene and precompressed glass-fiber, showed that the dynamic stiffness of all measured mounts increases with increasing static load. The dynamic stiffness was found to be independent of frequency in the region from 20 Hz to 2 kHz. A comparison of the static load-deflection curves[a] with the curves of dynamically measured stiffness indicates that the tangent of the static load-deflection curves does *not* agree with the measured dynamic stiffness. The tangent of the static load-deflection curve for every type of mount indicates stiffness two to three times smaller than the stiffness measured dynamically. Both the static and the dynamic stiffness of the cork mounts show an anisotropic behavior. The static load-deflection curve of the cork

[a]The static load-deflection curves were measured by the Korfund Dynamics Corporation.

samples would also indicate a dynamic softening of the mount with increasing static load – an indication disproved by the dynamic measurements.

A sample calculation of the improvement in sound and vibration isolation achieved by a resiliently supported floating slab indicates that, above the basic resonance frequency of the system, the improvement increases with increasing frequency at the rate of 30 dB/decade. For a given floating floor system, the improvement in air-borne sound isolation is practically the same as the improvement in vibration isolation. The calculations point out the importance of a high loss factor for both the acoustical and the vibrational performance of a floating floor system.

Calculation of the *flanking* sound transmission between the source and receiving room shows that the large potential improvement in transmission loss for air-borne sound, to be expected from the addition of a floating floor, cannot be realized in practice unless one also reduces the flanking transmission. On the other hand, since a properly installed floating slab had no rigid connections to the walls of the source room, its vibration isolation performance remains practically unaffected by flanking through the walls.

Figure 21 illustrates the proper use of a floating floor in a typical mechanical equipment room. The airspace between the structural slab and floating slab is filled with low-density non-load-bearing glass-fiber, designed to reduce the dynamic stiffness of the trapped air.[a] Machines with a disturbing frequency

[a] For isothermal processes $\gamma = 1.0$, compared to 1.4 for adiabatic processes; this result of adding the glass-fiber is an apparent increase of about 40% in the volume of the airspace, even though the glass-fiber itself occupies some of the volume.

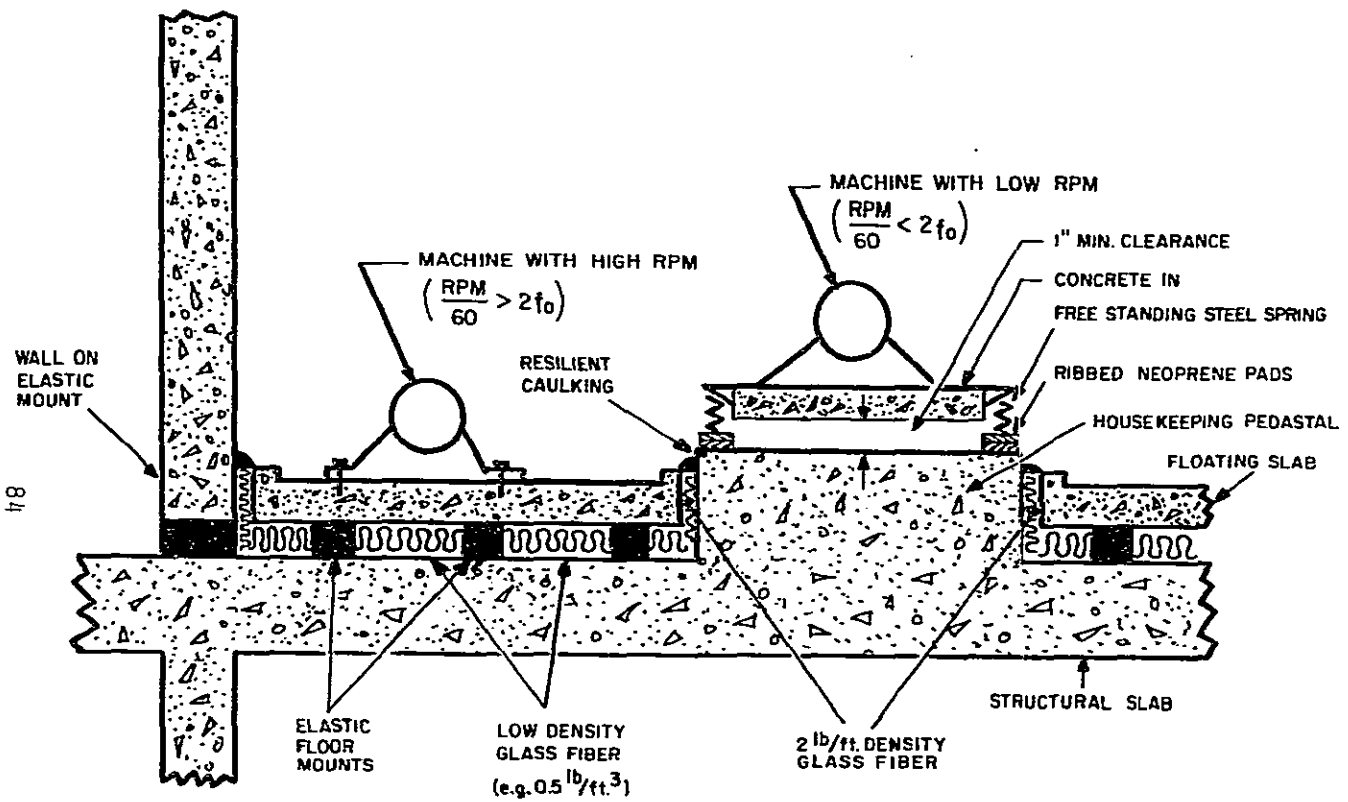

FIG. 21 ILLUSTRATION FOR THE PROPER USE OF FLOATING FLOORS

(RPM/60) lower than twice the basic resonance frequency, f_0, of the floating floor system (as given in Eq. 14) will require independent treatment, they should be bolted to a heavy concrete inertia block resting on steel springs in series with two layers of ribbed neoprene, supported on a housekeeping pedestal. The housekeeping pedestal should be somewhat higher than the level of the floating slab. Machines with disturbing frequencies above $2f_0$ can either be rigidly mounted on the floating floor as shown in Fig. 21, or may need additional vibration isolation. The choice of the mounting depends on the degree of vibration isolation required.

The air gap around the perimeter of the floating slab and also around the housekeeping pedestal should be cleaned, filled with low-density glass-fiber (0.5 lb per ft^3), and caulked with a non-hardening caulking compound. This treatment is absolutely essential, to reduce flanking transmission of vibration from the floating slab to the walls.

In order to protect the vibration mounts and the glass-fiber in the airspace from water, the floating slab should have a rim around the perimeter, as shown schematically in Fig. 21. If possible, no pipes or ducts should penetrate the floating floor. When penetrations are unavoidable, carefully detail them to avoid short-circuiting the floating floor.

In order to realize the potential improvement in air-borne sound isolation expected from the floating floor, one must interrupt the flanking path through the mechanical equipment room walls. This can be done either (1) by setting the walls on a layer of vibration isolating material, such as cork, neoprene, etc. (as shown in Fig. 21), or (2) by erecting a second gypsum board or similar wall on the floating slab itself, which would protect the primary walls from incident sound. When a large improvement is sought, the ceiling must also have similar protection.

BBN has frequently used the second method in the design of music buildings; but we have found this method to be both expensive and impractical for mechanical equipment rooms, where the walls are penetrated in many places by pipes and ducts. Because of its simplicity, the first method seems to be better suited for mechanical equipment room applications than Method 2. Unfortunately, the scope of the present work did not permit us to assess the increase in flanking transmission loss due to the resilient supporting of the walls. Since the acoustical performance of a floating floor depends entirely on how well one controls the flanking, further study of the reduction of flanking transmission by resiliently supported walls is strongly recommended. The simplest approach would be experimental evaluation.

REFERENCES

1. Beranek, L.L., ed. *Noise Reduction*, McGraw-Hill Book Co., Inc., New York (1960).

2. Lyon, R.H., "Random Noise and Vibration in Space Vehicles", The Shock and Vibration Information Center, United States Department of Defense, 1967, SVM-1.

3. Morse, P.M. *Vibration and Sound*, 2nd ed., McGraw-Hill Book Co., Inc., New York (1948), p. 384.

4. Maidanik, G., "Response of Ribbed Panels to Reverberant Acoustic Fields", *J. Acous. Soc. Am.* 34, No. 6, 809-826 (1962).

5. Cremer, L. and M.A. Heckl, "Körperschall", Springer Verlag, Berlin/Heidelberg/New York (1967), p. 273.

6. Meyer, E., P.H. Parkin, H. Oberst, and H.J. Purkis, "A Tentative Method for the Measurement of Indirect Sound Transmission in Buildings", *Acustica* 1, p. 17 (1955).

7. Westphal, W., "Ausbreiburg von Körperschall in Gebäuden", *Acustica*, Akustische Beihefte, p. 335 (1957).

8. Kihlman, T., "Transmission of Structure-borne Sound in Buildings", Report 9, The National Swedish Institute for Building Research, P.O. Box 27163, Stockholm 27, Sweden (1967).

9. Gösele, K., "Untersuchungen zur Schall-Längsleitung in Bauten", *Schallschutz in Gebäuden*, Heft 56, p. 25 (1968).

APPENDIX I: DESCRIPTION OF THE TESTED SAMPLES

A. Cork Mounts

The samples were cut from a large block made of pure granules of cork, compressed and baked under steam pressure at a steam temperature of 600°F without the addition of any foreign binder. The physical properties are controlled by granule size and density.

The density designation and load bearing capacity range for the different cork samples are:

DENSITY DESIGNATION		LIGHT	STANDARD	HEAVY
Specific weight	lb/ft^3	6.7/7	15/16	18/20
Load capacity	lb/ft^2	400–1400	1400–4300	4300–8000
Range	psi	2.78–10	10–30	35–55

B. Neoprene Mount

The mounts are made of neoprene, specially compounded to meet the requirements for elastomeric bridge bearing pads and cured for 30 minutes at 300°F. They have the following performance specifications:

1. Original physical properties:
   - 1.1 Hardness (Shore A) (ASTM D-676) ..... 60±5
   - 1.2 Tensile strength (min) (ASTM D-412) ..... 2500 psi
   - 1.3 Elongation at break 350%
2. Accelerated tests to determine long-term aging characteristics:
   - 2.1 Oven aging – 70 hours at 212°F (ASTM D-573)
     Hardness points change, maximum ..... 0 to +15

Tensile strength, percent change, maximum ... ±15
Elongation at break, percent change, maximum. -40

2.2 Ozone (1 PPM in air by volume — 20% strain — 100°F) (ASTM D-1149)
100 hours ..... no cracks

2.3 Compression set (22 hours at 158°) (ASTM D-395, method B)
Percent maximum 25

2.4 Low temperature stiffness (ASTM D-797)
At -40°F Young modulus, maximum ..... 10,000 psi

2.5 Tear test (ASTM D-624-DIE "C")
pound/lin in., minimum 225

3. The pad is of the compound known as neoprene cast in mold under pressure and heat. It is in accordance with the requirements of ASTM method D-15, Part B.

C. Precompressed Glass-Fiber Mount

The precompressed glass-fiber pad, of 2 in. × 2 in. × 2 in. dimensions, was supplied by the Korfund Dynamics Corporation and is believed to be equivalent to the "Q"-PAD of the Consolidated Kinetics Corporation.

APPENDIX II: CALCULATION OF THE FLANKING TRANSMISSION LOSS

The flanking sound transmission loss is defined as

$$TL_f = 10 \log \frac{\pi_0}{\pi_f} , \qquad \text{(II-1)}$$

where π_0 is sound power incident on the flanked wall from the source room, and π_f is the sound power radiated into the receiving room through the flanking wall.[a]

In a diffuse sound field the sound power incident on a wall of surface area A is given by:

$$\pi_0 = \frac{\langle p_1^2 \rangle}{4\rho_0 c_0} A . \qquad \text{(II-2)}$$

The normal sound transmission loss of the flanking wall is given by

$$TL_{NG} = 10 \log \frac{\frac{\langle p_1^2 \rangle}{4\rho_0 c_0} A}{\langle v_1^2 \rangle \rho_0 c_0 A \, \sigma_{rad_{NG}}} , \qquad \text{(II-3)}$$

where $\langle p_1^2 \rangle$ is the space-average mean square pressure in the receiving room, $\langle v_1^2 \rangle$ is the space-average mean square velocity of the flanking wall in the source room, $\sigma_{rad_{NG}}$ is the radiation efficiency of the flanking wall, and A is the wall surface area.

---

[a] In this derivation we assume that the flanking partition is a single wall.

Solving Eq. II-3 for $\langle v_1^2 \rangle$ gives

$$\langle v_1^2 \rangle = \frac{\langle p_1^2 \rangle}{10^{\frac{TL_{NG}}{10}} \left[4(\rho_0 c_0)^2 \ \sigma_{rad_{NG}} \right]} . \qquad \text{(II-4)}$$

The velocity transmission factor, γ, is defined as

$$\gamma = 10 \log \frac{\langle v_1^2 \rangle}{\langle v_2^2 \rangle} , \qquad \text{(II-5)}$$

where $\langle v_2^2 \rangle$ is the space-average mean square velocity of the flanking wall in the receiving room.

Solving Eq. II-5 for $\langle v_2^2 \rangle$ gives

$$\langle v_2^2 \rangle = \frac{\langle v_1^2 \rangle}{10^{\frac{\gamma}{10}}} . \qquad \text{(II-6)}$$

The power transmitted through the flanking walls is

$$\pi_f = \langle v_2^2 \rangle \rho_0 c_0 \sigma_{rad_{NG}} A_{NG_{RR}} , \qquad \text{(II-7)}$$

where $A_{NG_{RR}}$ is the total surface of flanking walls in the receiving room.

Using Eqs. II-4 and II-6, we get

$$\pi_f = \frac{\langle p_1^2 \rangle}{4\rho_0 c_0} \frac{A_{NG_{RR}}}{10^{\frac{TL_{NG}}{10}} \ 10^{\frac{\gamma}{10}}} . \qquad \text{(II-8)}$$

Combining Eqs. II-8, II-2, and II-1 yields

$$TL_f = 10 \log \frac{\pi_0}{\pi_f} = 10 \log \frac{\frac{\langle p_i^2 \rangle}{4\rho_0 c_0} A_0}{\frac{\langle p_i^2 \rangle}{4\rho_0 c_0} \frac{A_{NG_{RR}}}{10^{\frac{TL_{NG}}{10}} 10^{\frac{\gamma}{10}}}}, \qquad \text{(II-9)}$$

or,

$$TL_f = TL_{NG} + \gamma + 10 \log \frac{A_{KD}}{A_{NG_{RR}}} \qquad \text{(II-10)}$$

where A_{KD} is the surface area of the flanked wall.